Universidade do Minho
Escola de Engenharia

Cristina Santos Silva

Wear behavior of glass-ceramic and polymer-infiltrated ceramic materials for dental applications

26 de fevereiro de 2018

Universidade do Minho
Escola de Engenharia

Cristina Santos Silva

Wear behavior of glass-ceramic and polymer-infiltrated ceramic materials for dental applications

Dissertação de Mestrado
Mestrado Integrado em Engenharia Biomédica
Ramo: Biomateriais, Reabilitação e Biomecânica

Trabalho efetuado sob a orientação de

Professor José Gomes
Professor Júlio Souza

ACKNOWLEDGMENTS

First of all, I would like to thank my supervisor, Prof. José Manuel Ramos Gomes, for the support, dedication, patience, flexibility, guidance, encouragement and transmitted knowledge throughout the project. This work would not be possible without your cooperation and without your constant incentives. It was a real pleasure to work with you, I'm very grateful.

Also, to my co-supervisor, Prof. Júlio Souza that despite being far always counterpoised this distance in the progress of this work. Thank you for all the guidance and all the support.

To Doctor Antônio Pedro Novaes Oliveira, who offered sample materials, allowing the realization of the present study, thank you for the overall contribution.

To Engineer Sergio Carvalho for the excellent technical assistance and the constant words of support and encouragement in the less good hours, was fundamental for the accomplishment of this work. It was a pleasure working with you.

To Doctor Bruno Henriques for all the cooperation and support and help with the preparation of the samples for the tribological tests.

A thank you to all my friends, for supporting me at this stage, for being patient and listening to my worries, and for always be willing to put a smile on my face. Special thanks to Daniela Martins, for being a fundamental pillar throughout the master's degree, I would not be the same without your company, support, patience, understanding, and help.

Finally, I want to especially thank my parents, that always dedicated themselves to offering me the best possible opportunities of education and encouragement to pursue what I want and what I love to do, and never letting me down when I failed. All of this would not be possible without your help and sacrifice. Thanks for everything.

This work was supported by the Portuguese Foundation of Science and Technology through the projects: POCI-01-0145-FEDER-006941 and UID/EEA/04436/2013.

ABSTRACT

Wear of teeth and restorative materials has been often reported by general dental practitioners and researchers. Wear can occur at tooth-tooth, restoration-tooth, or restoration-restoration contacting surfaces, depending on the properties of the related synthetic and natural materials. All-ceramic restorations are the most popular type of dental restorations due to their optical and mechanical properties. However, the abrasiveness of ceramic materials results in progressive wear of contacting surfaces such as resin composite or tooth enamel. Concerning aaesthetics, strength, and wear, new glass ceramics and composites have been commercially introduced in the field of dentistry.

The objective of the present work is to study the tribological behavior of a zirconia-reinforced lithium silicate glass-ceramic and a polymer-infiltrated ceramic. Samples were tested on a reciprocating ball-on-plate tribometer at 30 N applied load, 1 Hz and stroke length of 2 mm. The wear sliding tests were carried out against an alumina ball in artificial saliva at 37 °C. Additionally, micro-scale abrasion tests were also performed in the presence of abrasive particles to simulate three-body abrasion conditions. The micro-scale abrasion tests were performed at 60 rpm with a normal load of 0.8 N for 600 revolutions of a stainless-steel ball in contact with a suspension of hydrated silica particles. After wear tests, the worn surfaces were inspected by scanning electron microscopy (SEM) and Energy-Dispersive Spectroscopy (EDS).

The main wear mechanism found during the tests was abrasion. However, the hybrid ceramic, during the reciprocating tests, presented an unstable adhesive tribo-layer, associated with a delamination process. Congruently, the wear volume obtained during the micro-abrasion tests were higher for the polymer infiltrated ceramic than for the glass-ceramic, $1.44x10^{-1}$ $mm^{3,}$ and $9.89x10^{-2}$ mm^3, respectively. The same happened to the specific wear rate for sliding tests where the hybrid ceramic obtained $5.33x10^{-5}$ $mm^3/N.m$ and the glass-ceramic $3.17x10^{-5}$ $mm^3/N.m$.

For all test conditions, zirconia reinforced glass-ceramic, presented higher wear resistance than hybrid ceramic, combined with lower friction coefficient against alumina, which indicates the potential of this reinforced glass-ceramic for application in dental restorations.

RESUMO

O desgaste dos dentes e materiais de restauro, tem sido referenciado muitas vezes por médicos dentistas e investigadores. O desgaste pode ocorrer na interação de superfícies em contacto, dente-dente, restauro-dente, ou mesmo restauro-restauro, dependendo das propriedades dos materiais sintéticos e naturais. Os restauros totalmente cerâmicos são o tipo mais popular de restauros dentários, devido às suas propriedades óticas e mecânicas. No entanto, a abrasividade dos materiais cerâmicos resulta no desgaste progressivo das superfícies em contacto como resinas compósitas ou esmalte dentário. Tendo em conta a estética, resistência e desgaste, novos vitrocerâmicos e compósitos têm sido introduzidos no campo da dentária.

O objetivo do presente trabalho é o estudo do comportamento tribológico de um vitrocerâmico de silicato de lítio reforçado com zircónia e de uma cerâmica infiltrada com polímero. As amostras foram testadas num tribómetro esfera-placa em deslizamento linear alternativo, com uma carga aplicada de 30 N, 1 Hz e 2 mm de amplitude. Estes testes foram realizados contra uma esfera de alumina em saliva artificial a 37 °C. Além disso, foram realizados testes de abrasão em micro-escala, na presença de partículas abrasivas para simular condições de abrasão a três corpos. Os testes de micro-abrasão foram realizados a 60 rpm e com uma carga normal fixa de 0,8 N para 600 rotações da esfera em aço, usando uma suspensão de sílica hidratada. Após os testes tribológicos, as superfícies desgastadas foram inspecionadas por microscopia eletrónica de varrimento (SEM) e por espetroscopia de energia dispersiva (EDS).

O principal mecanismo de desgaste encontrado durante os ensaios foi a abrasão. Porém, o cerâmico hibrido, apresentou uma tribo-camada adesiva e instável, associada a um processo de delaminação. Congruentemente, o volume de desgaste obtido durante os testes de microabrasão foi maior para o cerâmico infiltrado com polímero do que para o vitrocerâmico, $1{,}44\text{x}10^{-1}$ mm^3 e $9{,}89\text{x}10^{-2}$ mm^3, respetivamente. O mesmo aconteceu com a taxa de desgaste específica para testes de deslizamento em que a cerâmica híbrida resultou em $5{,}33\text{x}10^{-5}$ $mm^3/N.m$ e a vitrocerâmica $3{,}17\text{x}10^{-5}$ $mm^3/N.m$.

Para todas as condições de teste, o vitrocerâmico reforçado com zircónia apresentou maior resistência ao desgaste do que o cerâmico híbrido, combinando com menor coeficiente de atrito contra a alumina, o que indica o potencial de aplicação deste vitrocerâmico reforçado em restaurações dentárias.

TABLE OF CONTENTS

LIST OF FIGURES

LISTA OF TABLES

LIST OF ABBREVIATIONS

ISO	International Organization for Standardization
DEJ	Dentine-Enamel Junction
CAD	Computer-Aided Design
CAM	Computer-Aided Manufacturing
CTE	Coefficient of Thermal Expansion
Y-TZP	Ytria stabilized tetragonal zirconia polycrystal
CEREC	Chair-side Economical Restoration of Aesthetic Ceramics
ZLS	Zirconia reinforced Lithium Silicate
PMMA	Polymethyl Methacrylate
POM	Polyoxymethylene
ASME	American Society of Mechanical Engineering
DIN	German Institute for Standardization
VS	VITA Suprinity ®
VE	VITA Enamic ®
UDMA	Urethane Dimethacrylate
TEGDMA	Triethylene Glycol Dimethacrylate
FEGSEM	Field Emission Gun Scanning Electron Microscopy
SEM	Scanning Electron Microscopy
EDS	Energy Dispersive Spectroscopy
COF	Coefficient of Friction

LIST OF SYMBOLS

Symbol	Description
N	Normal load
E	Elastic modulus
R_a	Arithmetic average of roughness
R_q	Root mean square roughness
R_f	Maximum roughness
W	Load
F	Friction Force
μ	Friction coefficient
μ_s	Static Friction
μ_d	Dynamic Friction
θ	Semi-open angle of the asperity of harder material
S	Shear strength
σ	Yield stress
K	Wear coefficient
x	Sliding distance
K_{abr}	Wear coefficient by abrasion
b	Width of the wear track
S	Total sliding distance
L	Stroke length
ΔV	Total volume loss
c	Crater diameter
k	Specific wear rate

1. INTRODUCTION

1.1 Motivation

Teeth play a key role in overall nutrition and general health. However, clinical issues such as oral diseases, trauma, or other injuries such as wear, can occur. Wear is a natural and progressive phenomenon, that can result from physiological or pathological conditions such as dysfunctional occlusion or parafunctional habits leading to the enamel degradation. On teeth enamel, wear is more prevalent in individuals over age 30 [1–4].

The loss of tooth tissues is the most common clinical problem in dentistry, with multiple studies that estimate a prevalence of 97% in the population, where around 7% of the populations is requiring treatment, due to excessive dental wear [4,5].

Concerning such issues, there is a need to replace missing or damage teeth tissues, using partial or total restorations or even implants. Nonetheless, the introduction of new materials on the oral cavity brought up the other face of the clinical problem, that is dental wear. Wear of dental surfaces can occur on tooth-tooth, restoration-tooth, or restoration-restoration contacting surfaces and therefore that is closely dependent on the chemical and physical properties of the synthetic or natural materials [6–8].

Back in 1778, tooth degradation has initially provoked the interest of researchers and clinicians. However, only in the 1960s, attention turned to the tribological behavior of human teeth and the development of wear friendly materials with similar behavior to enamel. Since then, wear

of teeth and restorative materials has been the subject of many studies in the past decades given that it is a clinical problem that requires attention in the actual aging population [4,9,10].

The tribological study leads to a better understanding of wear behavior of biomaterials in the human body that is essential to develop dental materials with a long-term successful performance in the oral cavity. Accordingly, to ISO/TC 106 – Dentistry Standards, dental materials are required to be biocompatible, bond permanently to the tooth, match the natural appearance of tooth structure and other visible tissues, exhibit properties similar to those of tooth enamel. Regarding all the requirements, glass-ceramic and composite materials have been used in aesthetic restorative dentistry [3,4,11–14].

However, ceramics and glass-ceramics have a brittle behavior and low tensile strength, that lead to catastrophic brittle fracture under very low strain. Efforts have been made to produce reinforced ceramics with enhanced physical properties. In addition, the development of resin composites became more and more popular in dentistry due to the possibility of clinically handling. Also, polymer-based composite combines properties of ceramic and polymer to obtain materials whose performance and mechanical behavior is closer to those of teeth [2,15,16].

On the other hand, a lack of knowledge still exists in the tribological properties of novel glass ceramic and composite under different conditions as existing in the oral cavity. The wear behavior of contacting surfaces like enamel within a healthy state of occlusion and aaesthetics should be highlighted [1,7,8,17,18].

1.2 Scope and Aim of the Study

One of the most common procedures in dental practice is indirect restorations for replacement of lost or damaged dental tissues. Currently, ceramic-based materials are the choice for restorations due to their excellent optical properties associated with mechanical and biological properties suitable for this type of application [19].

Within several physical properties, wear resistance is of fundamental importance in the clinical performance of these materials when subjected to complex strains from chewing in the presence of food and abrasive substances. However, the mechanisms of wear of recent dental materials are still not well known [20].

In order to reduce the need for clinical trials, that are expensive and time-consuming, predictive laboratory tests, that mimic clinical failure modes, could be made. This type of experiments allows the extrapolation of the wear behavior of dental materials after introduction into the oral environment [21,22].

This master's dissertation aims to contribute to the knowledge of the wear behavior of new dental restorative materials, studying the tribological behavior of commercial zirconia-reinforced glass and polymer-infiltrated ceramics. Both materials were subjected to reciprocating sliding in artificial saliva, mimicking representative conditions of two-body wear under lubrication, as found in the mouth. In addition, micro-scale abrasion tests were performed in contact with hydrated silica slurry to simulate the three-body wear, that is similar to the tooth brushing procedure.

In this dissertation, a theoretical and experimental investigation in the field of biomaterials for glass-ceramic and composite dental restorations is presented. It is expected to raise special interest in the field of dentistry, given that the tribological behavior is essential to gauge the feasibility of materials for dental restorations.

1.3 Structure of the Dissertation

The text of this dissertation is structured in six chapters.

Within the first chapter, fundamentals are described revealing the importance of studying the tribological behavior of recent dental materials.

The second chapter describes the theoretical and bibliographical component of the two structures that intervene in the tribological processes in the oral cavity, namely tooth, and restorative materials. Also, the chronological evolution of the dental materials is analyzed, including technological improvements and new techniques of fabrication.

The third chapter deals with theoretical concepts regarding Tribology. Subjects such as friction, wear, and lubrication for dental applications are addressed, focusing on the tribological mechanisms in the oral cavity.

In the fourth chapter, the materials and methods of the present work are described, including the preparation and experimental procedures that were performed for tribological tests.

In the fifth chapter, the results and the discussion of this work are presented. At last, the sixth chapter reveals the final conclusions and some perspectives for future works.

2. TEETH AND RESTORATIVE STRUCTURES

2.1 Human Teeth

The human dentition consists of two sets of teeth. The first one is the set we start getting as an infant, this set of teeth also called as “milk” teeth or primary teeth. Later, those teeth are exchanged for the definitive dentition with the eruption of permanent teeth, that starts around 6 years old. From then until the child becomes 12 years old, all the primary teeth loosen and come out while the permanent teeth come through in their place. Up to the age of 13 years, the 28 out of 32 permanent teeth will appear [23].

Anatomically, the human mouth is divided into quadrants. Within each quadrant, there are four distinguish teeth groups: central and lateral incisors, one canine, first and second premolars, and the first, second and third molars, as shown in Figure 2.1 [24].

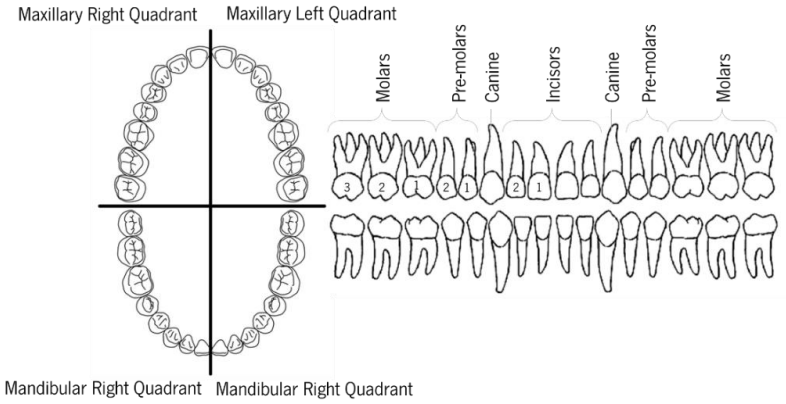

Figure 2.1: Structure and organization of human dentition, adapted from [25,26].

Each tooth consists of two parts, the section that is above the gum, named crown, and the root, which is integrated to the alveolar bone through the cementum and periodontal ligament. Human teeth have a unique structure composed of anisotropic tissues: enamel, dentine, cementum, and pulp. As seen in Figure 2.2, the outer layer of the crown is composed of an extremely hard mineralized tissue, named enamel, while the root is veneered by another mineralized tissue, known as cementum. The tissue layer below the enamel is named dentine, which comprises the bulk of tooth structure, and delimits the pulp cavity [27,28].

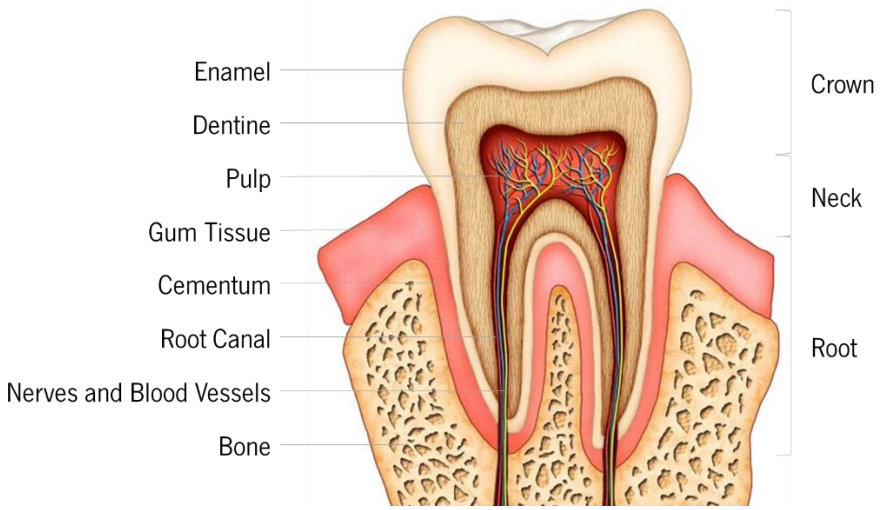

Figure 2.2: Tooth anatomy and tissues, adapted from [29].

The tooth pulp is a soft connective tissue formed from mesenchymal cells. The tooth pulp has a high density of nerves, blood vessels, and collagen fiber matrix and a high content of cells

like odontoblasts and fibroblasts. This tissue has a key role in the formation, sensing, nutrition, and healing of the dentin [28,30].

The cementum is a hard and complex tissue, that covers the dentine and anchors the root of the tooth in the alveolar bone on the jaw, through a periodontal ligament. This tissue, which covers the root of the tooth, does not have either blood or lymphatic vessels. [31].

Dentine is composed of a mineralized connective tissue, formed by 70%wt. of mineral material, mainly hydroxyapatite and fluorapatite, 18%wt. organic matrix, formed by collagen fibers, and 12%wt. of water. In fact, dentine is a complex natural composite, due to the multipart anatomy and physiology of this tissue. Responsible for giving support to the integrity of enamel, the dentine is composed of an aggregate of dentinal tubes, that run through the entire dentinal substance. These narrow channels in the dental structure, are surrounded by a mineralized dentine material and are filled with odontoblastic extensions. The odontoblastic extensions are responsible for the perception of the temperature, pH, pressure, and loading oscillation [23,24,27,28].

In addition to promoting a pathway to the cells, the dentinal tubes also provide mechanical support to adjacent tissues and is mainly important in the nearest region of enamel, once it inhibits crack propagation under fatigue. This region is known as the dentine-enamel junction [31].

Enamel is the hardest tissue in the human body due to its mineralized structure. Unlike other mineralized tissues, enamel does not present a collagen matrix in its composition. This tissue is formed by a unique extracellular matrix of ameloblasts, that synthesizes and secrete proteins. These cells form a protective thin layer that covers the enamel tissue, until the tooth eruption, and are central in the prevention of enamel flaws [23,24,30,32].

The enamel tissue is characterized by the presence of two structures, both composed of hydroxyapatite crystals. The enamel prisms, are a key-hole-shaped structure that radiates from the dentine-enamel junction and extends along the enamel tissue. The prisms are aggregate by another structure, the interprismatic enamel. Although these structures have the same composition, they differ in crystal orientation. These histologic arrangements confer the mechanical properties to the enamel tissue, shown in Table 2.1. Enamel reveals a stiffer and brittle behavior when compared to dentine (Table 2.1.) [28,31,33].

Table 2.1: Mechanical and physical properties of human tooth tissues [32-37]

	Hardness, (GPa)	Flexural Strength, (MPa)	Compressive Strength, (MPa)	Fracture Toughness, ($MPa.m^{1/2}$)	Young's Modulus, (GPa)	Density, (g/cm^3)
Enamel	3.03	141	10	0.77	94	2.97
Dentine	0.58	172	52	3.4	20	2.14

The properties of teeth tissue should be considered when restorative materials are used to replace missing structures. The understanding of mechanical properties of the natural tissues is determinant to improve the long-term success of restorative materials [34].

Restorative materials require proper adhesive bonding to dentine and enamel to establish the expected tissue replacement. Glass ceramics have a fracture toughness ranging from 1.0 up to 3.0 $MPa.m^{1/2}$, which is relatively close to the enamel fracture toughness of 0.77 $MPa.m^{1/2}$. Nevertheless, fractures of all-ceramic crowns are difficult to prevent due to the absence of a transition zone in mechanical properties between the restorative material and dentine. That leads to an abrupt change in stress distribution through the structures. The dentine-enamel junction (DEJ) in teeth is such transitional zone responsible for a smooth distribution of stresses [35,36].

On compressive stress, dentine can sustain significant plastic deformation on loading before fracture. Therefore, dentine is tougher than enamel. The elastic modulus (E) of enamel is approximately three to five times greater than that of dentine. Nevertheless, enamel and dentine work together during cyclic loading from mastication. Generally, interfaces between materials with dissimilar elastic and mechanical properties represent "weak links" in a structure, although the DEJ acts successfully to transfer forces from the enamel to the dentine and to inhibit crack propagation at the enamel and causing tooth fracture, even in cases of bruxism [35,37,38].

In human enamel and dentine, fatigue damage is the end result of extreme loads and is frequently associated with pathology or extensive wear. For the natural tooth, Zaslansky wrote, *"the asymmetry in stiffness between the buccal and lingual sides may, therefore, have a profound significance in determining how exactly the enamel cap responds to load during mastication"* [39]. This asymmetric nature of the structure may also contribute to the distribution of loads that are

not applied along the long axis of the tooth. The possible asymmetry in stiffness between the buccal and lingual sides of the tooth points to a basic property of tooth function, presumably related to the precise way that stress is distributed during mastication [40].

From there, we must find the balance between the natural tooth preparation, restorative material, the adhesive and the nature of the load. It is essential to find a methodology for analyzing the behavior of the teeth and materials to apply the physical principles for oral rehabilitation.

2.2 Restorative Materials

Regarding historic reports, bone and ivory and waxes, powdered pearl, gold, were used as dental restorative materials. It is possible to trace evidence for the use of alternative restorative materials from 3000 BC in Mesopotamia, where copper was used to cast. At 2500 BC, the Egyptians developed the wax molding process for gold casting. 2000 years later, Etruscans produced extracted teeth attached by using gold-based infrastructures. Even though some metals present physical properties proper for dental reconstructions, this class of materials has a serious problem associated with corrosion and biocompatibility in the oral cavity.

Metal-ceramic prosthetic structures combine the interesting optical properties of ceramics and the mechanical strength of metals. However, some metals used as restorative materials in dentistry can bring clinical issues for some patients, such as allergies [41], gum staining [42], and release of metallic ions into the oral cavity [43]. These major problems, as well as the search for more aesthetic materials, have created the need to develop metal-free prosthetic structures [44,45].

The increasing interest in aesthetic outcomes, associated with the need to use materials of excellent quality leads to the development of ceramic and composite materials. Ceramic materials have characteristics as color, texture, strength, chemical stability, abrasion resistance, and low coefficient of thermal expansion(CTE) compatible with the dental structures [46].

Porcelain was the first ceramic material to be introduced into dentistry. Despite being a well-known material and used in other areas since 300 AD, ceramics were only used in dentistry 1200 years later, as shown in Figure 2.3 [47,48].

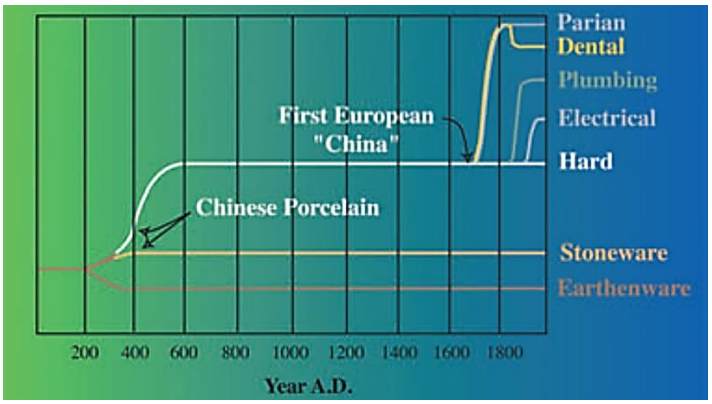

Figure 2.3: Porcelain history timeline [48].

The first record of ceramic prosthetic structures dates from 1774, when Alexis Duchateau and Nicholas Dubois, manufactured the first complete ceramic denture, using feldspar-based porcelain. It was only in the 19th century that Giuseppangelo Fonzi was capable of manufacturing individual ceramic teeth attached to a metallic substructure. Single unit all-ceramic prosthetic structures were accomplished in1837 when John Murphy developed the first ceramic inlay structure. Metal-free restorations boosted advances in the development and manufacture of dental ceramics [48,49]. Porcelain materials have shown variation in chemical composition involving feldspar, kaolin, and quartz preponderant, as represented in Figure 2.4.

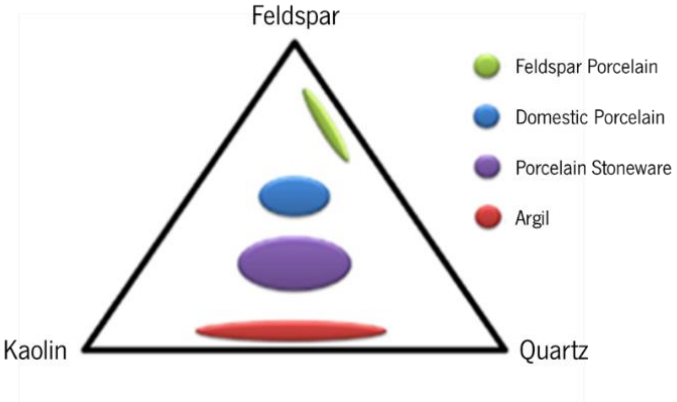

Figure 2.4: Composition of different porcelains [50].

Feldspar-based porcelains present translucency and CTE similar to those of the teeth. These materials are also resistant to compression and hydrolytic degradation in the oral cavity. On the other hand, they have low tensile and flexural strength and high hardness. These ceramics have also limited plastic deformation capacity and high elasticity modulus [51].

Despite the aesthetic potential and biocompatibility of feldspar-based ceramics, these materials are fragile, with low tolerance to tensile and shear stresses. Such glass ceramic materials are subjected to the formation and propagation of cracks due to their low fracture toughness. Therefore, cracks can appear after the manufacturing by thermal treatment as a result of residual stresses during cooling. On loading, the presence of cracks can lead to a catastrophic fracture of the material [52].

Following the evolution of restorative materials, several ceramic systems were introduced in the market between the end of the last century and the beginning of this century. The technological development of ceramic restorative materials follows the continuous search for desirable aesthetic outcomes. Consequently, there is a need for the evolution of manufacturing technique and equipment [53].

Ceramics are inorganic, non-metallic materials, which are typically composed of a bonding between metallic and nonmetallic elements such as aluminum & oxygen (alumina - Al_2O_3), calcium & oxygen (calcia - CaO), silicon & nitrogen (silicon nitride- Si_3N_4) [54]. Ceramics used in dentistry usually present a crystalline and a glassy phase in their microstructure. Crystalline phases such as leucite, lithium disilicate, alumina, and zirconia are the most commonly used as strengthening agents of the ceramic microstructure [6,51].

The first dental ceramic material to receive this kind of structural strengthening treatment was the feldspar-based porcelain. McLean and Huges developed a feldspar-based porcelain with a higher content of alumina oxide. Increasing the amount of alumina was able to decrease the concentration of stresses inside the material. Even though this material was considered more aesthetic than the metal-ceramic structures, the strength of the reinforced porcelain was still low concerning the mastication loading on posterior regions in the mouth. [55].

Factors such as crystal size and geometry, modulus of elasticity, phase transformation and thermal expansion mismatch between crystal and glassy phase have a preponderant role in the performance of the material. When it comes to all-ceramic systems it should be kept in mind that some extrinsic factors such as working conditions play a major role in the long-term performance of the material. Regarding dental materials, the oral environment gathers a set of challenging working conditions such as humidity, a variation of pH and cyclic loading [56].

Advances in the formulations of dental ceramics introduced ceramic systems infiltrated with a glassy phase. Those ceramics were indicated for restoration of total crowns in the anterior and posterior regions due to their improved mechanical strength. Emerging ceramic materials reinforced by the increase of 55%wt. leucite crystals resulted in an increase in fracture toughness. However, the shrinkage of leucite-reinforced glass ceramics was a limitation concerning the fitting of ceramic crowns to teeth structures. Regarding issues on leucite-reinforced porcelains, glass-ceramics containing 60 to 65%wt. lithium disilicate crystals were developed for inlays, onlays, and anterior crowns, Figure 2.5 [53,56,62].

Figure 2.5: Types of dental restorations [57]

Glass-ceramics reinforced by lithium disilicate shows both fracture toughness and flexural strength around three times higher than that for feldspar-based porcelains. Due to the favorable translucency, these glass-ceramic materials can be used for fully anatomic monolithic crowns for incisors and pre-molars [48,51,58,59]. The long-term success rate of reinforced glass-ceramics presented long-term survival is around 95-98 % for 5 years [60,61].

For approximately 10 years, Computer-Aided Design/Computer-Aided Manufacturing (CAD/CAM) techniques have become established in dentistry. During the development of CAD/CAM technology, new materials were also developed for digital dentistry over time, to respond to the traditional dental ceramics problems, such as low fracture toughness and catastrophic fracture [62].

The improvement of mechanical strength of glass-ceramics depends on the shape, size, content and chemical composition of the crystals. The commercial material Vita Suprinity ® (Vita Zhanfabrik, Germany), represents a new generation of zirconia-reinforced lithium silicate glass-ceramic material, that combines the positive material characteristics of zirconia (ZrO_2) and glass-ceramic, once the structure, after crystallization, exhibits excellent mechanical properties and meets the highest aesthetic requirements [59,63–65].

These microstructural phases influence the properties of the materials, since the crystalline phase is responsible for the mechanical strength, preventing the formation of cracks. In turn, the glassy phase controls the translucency and wear resistance aspects. The increase in glassy phase provides higher translucency while the crystalline material will result in high opacity. Also, the optical properties depend on the size, density, and porosity of the crystalline phase. Such relationship is illustrated in Figure 2.6 [50,59].

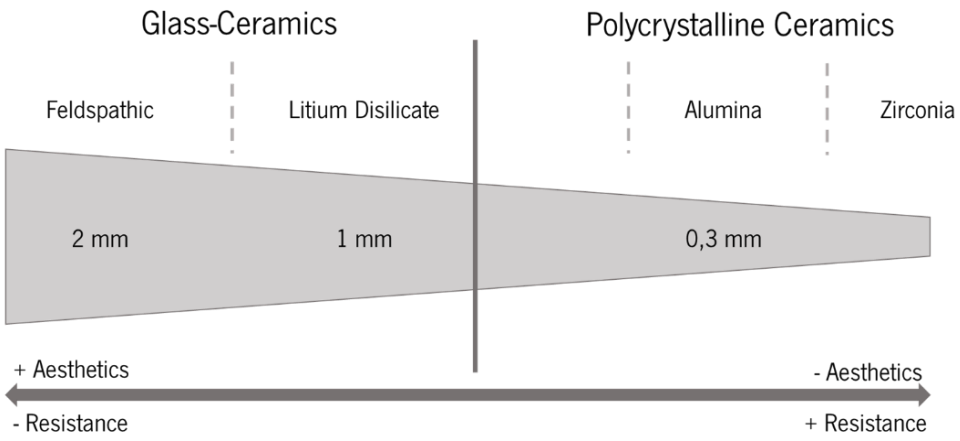

Figure 2.6: Relation between aesthetic properties and mechanical strength of materials with different compositions, diagram adapted from [50].

The overall structure and the glassy and crystalline phases, of the zirconia-reinforced lithium silicate glass ceramic material, guarantee a consistently high load capacity, as well as long-term reliability for the ceramic structure preventing the crack propagation. In the other hand, this material was recently introduced in the market, so there is not a lot of information about the performance *in vitro* and *in vivo* [65].

Yttria-stabilized tetragonal zirconia polycrystal (YTZP) has also been used to manufacture crowns. This material was initially used in the preparation of orthopedic prostheses due to its excellent mechanical properties and biocompatibility. In dentistry, YTZP is indicated for the manufacturing of total crowns and fixed partial prosthetic infrastructure for anterior and posterior regions. YTZP infrastructures are veneered with glass-ceramic to mimic the optical properties of the teeth structures [48,51,58].

Comparing different clinical studies, all-ceramic systems have revealed global survival rates ranging from 88 up to 100 % after 2 years while 84-97 % is achieved after 5 to 14 years. Despite the wide range of materials, there is not any ceramic combination that replicates the mechanical

behavior of the teeth. Ceramics can also promote excessive wear of counter bodies such as enamel and other restorative materials during occlusion and mastication [66–73].

In fact, composites are a good strategy to combine the advantages of ceramic and polymeric materials concerning mechanical behavior, wear and optical properties. Polymer infiltrated ceramic network consists of a hybrid material with both polymer and ceramic interpenetrating networks. A commercial material namely Vita Enamic ® (Vita Zhanfabrik, Germany) is composed of a acrylate polymer network embedded with an conventional feldspar glass-ceramic [74].

This hybrid ceramic, shows flexural strength, hardness, and elasticity close to that recorded for dentine, combined with the long-lasting aaesthetics of ceramics. However, long-term *in vivo* studies are still in progress, and even *in vitro* studies are scarce, so there is still not enough data to predict the overall performance of this material in the oral cavity [75–79].

2.3 CAD/CAM Technology in Dentistry

After decades of evolution, contemporary dentistry has increasingly employed conservative, minimally invasive, restorative procedures, which include indirect procedures such as the fabrication of the restorations. The technological changes taking place are truthfully revolutionizing the way dentistry is practiced. The advent of CAD/CAM has enabled the dentists and laboratories to join the power of computers to design and fabricate aesthetic and more reliable dental restorations [80].

Duret introduced, for the first time, the concept of dental CAD/CAM back in 1971. The need for a uniform material quality, reduction in production costs, and standardization of the manufacturing process has encouraged researchers to seek to automate the conventional manual process via the use of this technology since the 1980s [81]. In 1987, Mörmann and Brandestini introduced a prototype machine that would capture a three-dimensional (3D) image of a prepared tooth. This system became known as Chair-side Economical Restoration of Aesthetic Ceramics (CEREC), one of the most used dental CAD/CAM system [82,83].

Although there are different CAD/CAM systems, all follow the same chain process of scanning, designing, and milling phases [84]. CAD/CAM technology may also be classified accordingly with manufacturing techniques. The processes described can be synthesized in the diagram of Figure 2.7.

Dental CAD/CAM technology was originally intended for hard machining of the fully

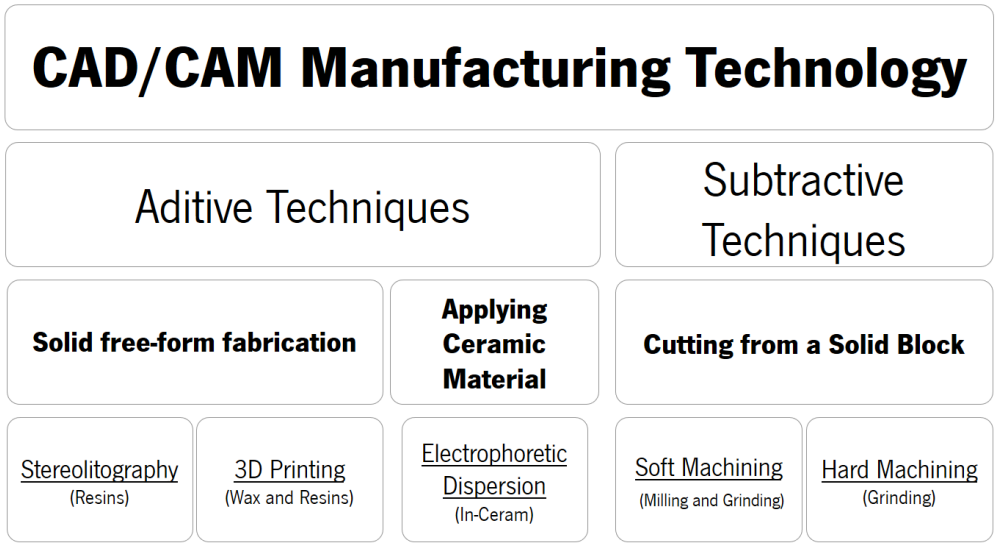

Figure 2.7: Overview of CAD/CAM manufacturing systems for dentistry, diagram adapted from [85]

sintered ceramic block and has now been expanded for partially sintered ceramics, appearing the concept of soft machining, where the restorations undergo a heat treatment to ensure adequate and full sintering [85].

Early materials, used in hard machining, included Fluor-rich mica glass-ceramic. This material exhibited a classic "house of cards" microstructure due to the interlocking mica platelets. Those cleavage planes offered by the mica crystals gave the ceramic an excellent machinability. Then, a wide range of ceramic materials is available for CAD/CAM hard machining, since feldspar-based, leucite-based up to lithium disilicate-based ceramics. Currently, not only ceramics might be manufactured by hard or soft machining. Some temporary and even permanent dental restorations can be milled of polymeric CAD/CAM blocs, materials such as polymethyl methacrylate (PMMA)-based or polyoxymethylene (POM), and even some hybrid composites. Being that restorations milled of PMMA-based CAD/CAM blocks present better mechanical properties, good translucency, and a higher stability against discoloration compared to the conventionally polymerized ones [86–91].

It's important to note that the material used depends on functional and aesthetic demands and on whether a chair-side or in-lab CAD/CAM restoration is fabricated. For chair-side CAD/CAM restorations, an aesthetic, strong material requiring minimal post-milling aesthetic adjustment to minimize the chairside time is needed. For these reasons, formulations were quickly developed

such as strengthened and fine-grained feldspathic ceramics, and reinforced glass-ceramic, that were introduced more recently [48,92].

The traditional methods of dental restoration manufacture are known to be time-consuming, technically sensitive and unpredictable. For that reason, by using CAD/CAM restorative techniques, some steps of the traditional manufacturing techniques can be simplified or even eliminated [80,84,89,92].

Another problem associated with manual restoration manufacturing is the poor marginal adaptation of restorations that leads to the increase of plaque retention, carrying potentially secondary caries and periodontal diseases. The accuracy-compromising aspects of CAD methods such as data collection, locating the margin in the digital representation, and restoration design, associated with CAM techniques, are some of the toughest challenges, especially for brittle ceramics. The machinability of these materials can compromise the accuracy of the restoration fit, the regularity of the surface, and the shrinkage associated with post-machining sintering of the partially sintered blocks. Despite all these small problems that can be somehow managed, CAD/CAM restorations still present better accuracy and overall results [21,62,93].

CAD/CAM restorations present a natural appearance due to the translucent quality of the ceramic blocs, that emulate enamel. The chances of success are, therefore, as high as those with conventional veneers, once 98.8% of patients describe their CAD/CAM-produced solution as successful. Finally, quality is consistent because prefabricated ceramic blocks are free from internal defects and the computer program is designed to produce shapes that will stand up to wear [19,83].

Advances in CAD/CAM technology have catalyzed the developments of aesthetic all-ceramic restorations with superior biomechanical properties. The field of CAD/CAM ceramics in dentistry is strongly evolving with evidence from materials development and from longer-term clinical studies [89].

Challenges remain in both understanding and improving the clinical performance of dental restorations. These include improved consistency and breadth of information about factors in clinical studies, definition of failures, and laboratory testing procedures. In parallel, developments in numerical analysis, physical properties of materials, and fabrication approaches all hold promise.

3. WEAR IN THE ORAL CAVITY

3.1 Wear - Historic Contextualization

The science of the interaction between materials under relative contact action is named *Tribology*. This word derives from the Greek *tribos*, meaning rubbing, and the suffix *logos* which means study. The literal translation would be "The science of rubbing". Tribology is a multidisciplinary science, which encompasses areas such as mechanics, physics, chemistry, and material science. Tribology also performs operational analysis of problems like reliability, wear, and maintenance, ranging from the shoes to spacecraft issues [94,95].

In order to understand the mechanisms of surface interactions, tribology requires knowledge of various disciplines such as rheology, mathematics, materials science, lubrication, thermodynamics, and much others, depending on the tribological system [96].

The term tribology is relatively new, being introduced in 1966, in a report by Professor H. Peter Jost from the Department of Education and Science in the United Kingdom. On the other hand, tribology cannot be considered a new field, once friction is part of human history since the Paleolithic period from the preparation of fire and drilling holes. In a tomb at Saqqara, an Egyptian illustration of the transport of the Ti statue shows a man lubricating sliding surfaces. This image shown in Figure 3.1, was then reported to be the image of the first tribologist [96,97].

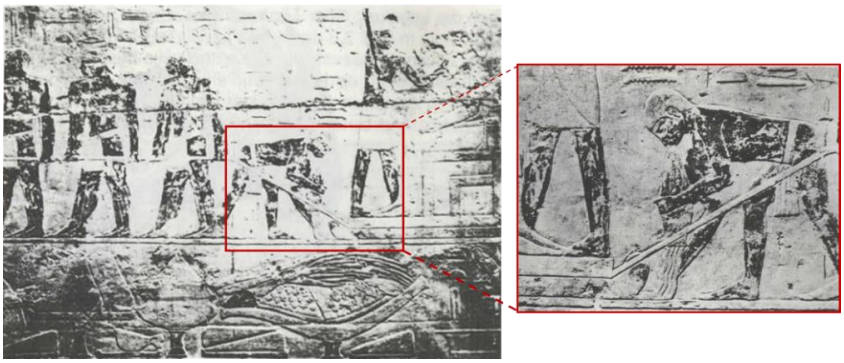

Figure 3.1: Transporting the statue of Ti, adapted from [96] and, [97].

During and after the Roman empire, engineers designed war machinery using tribological principles although the first scientific approach to friction was only formulated by Leonardo da Vinci (1452-1519) in the Renaissance period. According to da Vinci's findings and deductions, the frictional resistance was the same for two different objects of the same weight, even if they established contacts over different widths and lengths. Da Vinci observed that the force required to overcome friction increase two times in magnitude when the weight also increased two times. Although his work had no historical influence, da Vinci's findings remained unpublished for hundreds of years.

Many discoveries occurred during the 1500s, that is now applied in the resolution of tribological problems. The laws of viscous flow, postulated by Isaac Newton in 1668, and the improvements on bearing materials, proposed by Robert Hooke in 1684 [42–44].

Wear compared with friction, is a much younger subject of study, given that the scientific wear studies started around the mid-twentieth century. The interest in wear phenomena was triggered during the rapid industrial growth, impelling knowledge of all areas of tribology. One of the first substantial contributions in this area was given by Ragnar Holm at 1946 [97].

The increased emphasis on tribological concepts followed the huge costs with wear and corrosion problems in the British industry as published in "The Jost Report". As a result, several national centers of tribology were set up in the UK and elsewhere. Since then, the term was diffused into international engineering field and tribology has become a major part of applied sciences [100].

In 1969 the International Research Group on Wear of Engineering Materials put together a glossary of terms and definitions in the field of tribology. The glossary is included in the "Wear

Control Handbook" of the American Society of Mechanical Engineering (ASME), that defined wear as the progressive loss of substance from the operating surface of a body, occurring as a result of relative motion at the surface [101].

Recent advances from a theoretical and conceptual point of view, have shown a tremendous complexity in relation to what would seem to be the simplest tribological process. Since the appearance of new experimental methods from the 80's, the construction of the frictional model became more feasible [97,98,102].

With the miniaturization of components, the relationship between the area and volume has increased, what reveals more questions on the tribology in micro-scale systems. Phenomena such as adhesion are the object of study today, in multiples disciplines. There are different forms of wear according to different mechanisms of interaction between materials. However, there is no internationally accepted ISO standard norm on the different types of wear. A norm by the German Institute of Industrial Norms (DIN 50320) was withdrawn in 1997. In this norm, the following mechanisms were defined: Adhesion, Abrasion surface fatigue, and tribochemical processes, as described in Figure 3.2 [103–107].

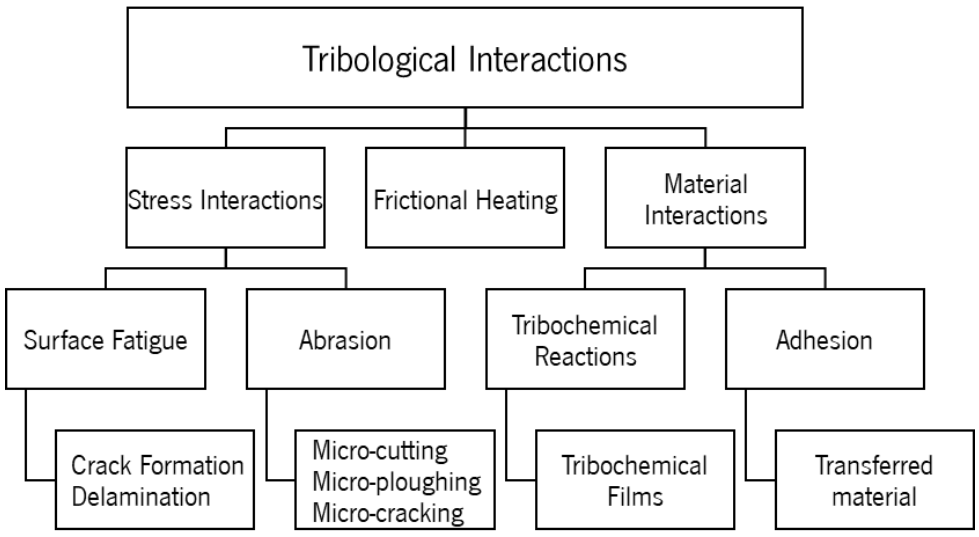

Figure 3.2: Tribological interactions and wear mechanisms [107]

3.2 Concepts of Tribology

Tribology is defined as "the science and the technology of surfaces that interact during relative motion", this involves friction, wear, and lubrification. These topics are widely associated with the properties of the involved materials, as well as the surface properties and the nature of the contact. Once, at a microscopic scale, there is none completely smooth surface. Although some surfaces could seem to be perfectly smooth, when observed through the microscope or with profilometry techniques, they reveal an aleatory distribution of peaks and valleys, forming the surface roughness, whose number and size determine the real contact area. The contact area between two surfaces without considering surface roughness concepts is named apparent contact area, whereas the real contacts between the tops of mating asperities give rise to the called real area of contact. Typically, the real area of contact is up to 1% of the apparent contact area [94,99,108].

Optical and mechanical methods can be used to measure the nano, micro or macroscopic geometrical characteristics of the surfaces. To characterize the topography of the surfaces, there are several statistical parameters, being the most common the center line average. This value of also called roughness R_a is the arithmetic average of roughness deviations from the mean line considering the dimensions of consecutive peaks and valleys. There are other parameters currently used, such as the root mean square, R_q, and maximum roughness, R_t, that is defined as the higher distance between the highest peak and deeper valley in the profile of roughness [94,99,108].

The function of the materials, the geometries and surface features, and roughness of the bodies in contact, as well as the operating conditions and environment, will influence the magnitude of the resistance to motion. This resistance to movement during sliding or rolling is named **friction**. This concept can be verified when one solid body moves tangentially over another one with which it is in contact, illustrated in Figure 3.3. The tangential force (F), which acts in opposition to the direction of the movement, is named friction force [102].

In 1699, Guillaume Amontons proposed two laws of friction. The first one, tells that the friction force is independent of the apparent contact area between the two bodies, and the second law, says that the friction force is directly proportional to the surface-normal component of load [94]. The second law gives us the Equation 3.1:

$$F = \mu \times W \tag{3.1}$$

Where F is the friction force, W is the load and μ is the friction coefficient [94,109]. To understand this relationship, consider the inclined plane experiment shown in Figure 3.3.

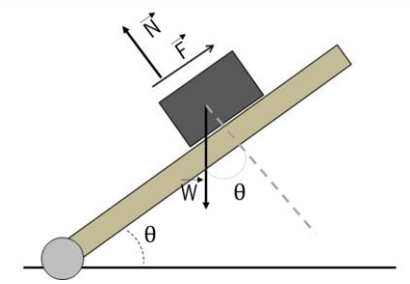

Figure 3.3: Illustrative representation of the force diagram in a sliding motion, adapted from [102]

As the plane is tilted up, the inclined angle θ is increased, and the component of the force due to the weight of the block in the direction of sliding increases. The friction coefficient, which is the ratio of the friction force F to the normal force W, is simply equal to tan θ [102]. Thus, the magnitude of the friction before sliding begins is usually greater than that during sliding. Therefore, friction can be the force which resists movement (dynamic friction) or the force that avoid the movement (static friction) [94,110]. The dynamic friction is usually somewhat smaller than the static friction, and this relation may be seen in Figure 3.4. The static friction is defined as the coefficient of friction corresponding to the maximum force that must be overcome to initiate macroscopic motion between two bodies. For a pair of materials tested under certain sliding conditions, the coefficient of friction tends to assume a steady mean value [94,109].

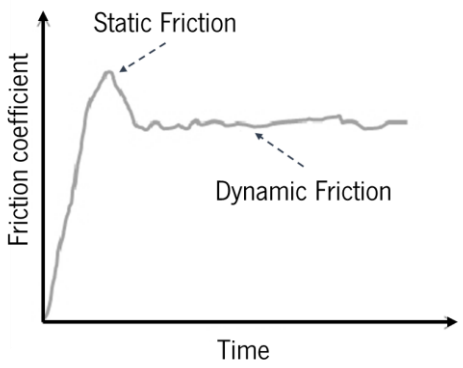

Figure 3.4: Friction coefficient evolution typical curve during sliding motion, adapted from [102]

A third law was then introduced by Coulomb, in 1785, stating that the friction force is independent of velocity once movement starts. However, experimental observations show that this statement is not always true as the friction coefficient could vary significantly with the variation of sliding speed. On the other hand, the frictional force necessary to initiate sliding is generally greater than that required to maintain it, and thereupon, the coefficient of static friction (μ_s) is greater than the coefficient of dynamic friction (μ_d). In many tribological systems, μ_d is found to be almost independent of velocity when this parameter varies in a short range of values, but when the velocity significantly increases for contacts involving metals, the friction coefficient usually decreases [110].

In non-lubricated sliding contact between two surfaces, friction may occur from a single or a combination of pathways, such as the adhesion between the protruding asperities of the mating surfaces. This adhesion theory of friction is based on the fact that the contact between surfaces is established only at the asperity peaks, being able to suffer elastic or plastic deformation, according to the intensity of normal applied load. In real contact zones, a strong adhesion between the mating surfaces occurs due to interatomic and intermolecular forces [111,112].

This theory predicts that the value of the coefficient of friction is associated with the mechanical properties of the contacting materials, being given by the Equation 3.2:

$$\mu = \frac{s}{\sigma} \tag{3.2}$$

Where μ is the coefficient of friction, s is the shear strength of the softer material involved in the contact and σ is the yield stress of the softer material [112].

The plowing mechanism of friction considers that a hard asperity is entrenched in the soft antagonist material and that it pushes the plastic flow of the soft material away to form a groove during sliding [111]. The resistance to sliding motion due to the penetration of the asperity in the opposing softer material defines the component of friction, gives in the Equation 3.3:

$$\mu = \frac{2}{\pi} cot\theta \tag{3.3}$$

Where, θ is the semi-open angle of the asperity of harder material, assuming a conical geometry for the asperities. This theory explains the friction phenomenon based only on the surface roughness of the harder surface of the sliding pair [110–112].

Friction depends on many parameters and therefore a mathematical formulation to estimate the friction coefficient for a given real sliding contact situation does not exist, being difficult to determine friction without experimental evaluation. However, the mentioned theories of friction constitute the basis for the understanding of the friction and wear phenomenon [111,112].

Wear, commonly defined as the progressive loss of surface material caused by mechanical and chemical action due to the contact and relative movement against a solid body, typically, is undesirable as it can lead to increased friction and ultimately to component failure. Still, it is a process that can be controlled, but not completely eliminated [97,98,102].

The usual mechanisms of wear are adhesion, abrasion, surface fatigue and tribochemical reactions. These mechanisms classify the process by which material is removed from the contact surface, promoting changes in the surface morphology and the generation of wear particles. The two most common types of wear are abrasive, in which a harder material removes material from a softer one, and adhesive, in which two bodies adhere to one another locally so that material is transferred from one to the other [94,99,108,109,111].

The adhesive wear is a surface degradation mechanism explained by the interatomic and intermolecular forces established between the asperities of two contacting surfaces at the real contact zones. Thus, there is the adhesion between mating asperities, occurring a temporary cold-welding phenomenon. Therefore, with the sliding motion of one mating surface against the other, the junctions previously established, by adhesion, disintegrate [111]. The volume loss of material, according to the formulation of this mechanism is given by the Equation 3.4:

$$V = K\frac{Wx}{3\sigma} \tag{3.4}$$

Where V is the wear volume, K is the wear coefficient, W the normal load applied, x the sliding distance and σ is the yield stress of the softer material of the contact [111].

Considering the expression 3.4, it is possible to define the three laws of wear:

I. the wear volume is proportional to the distance of sliding;
II. the wear volume is proportional to the normal load;
III. the wear volume is inversely proportional to the yield stress of the softer material.

When the transfer of material from the softer surface to the hardest one occurs by the agglomeration and adhesion of loose wear debris, tribochemical adherent films, or material directly transferred between the mating surfaces, this phenomenon gives rise to an adherent third body, Figure 3.5 [99,102].

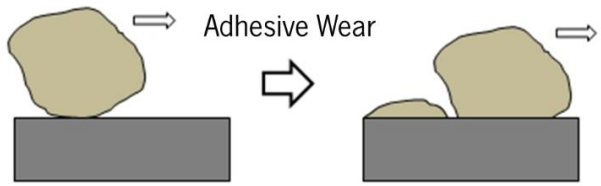

Figure 3.5: Representation of adhesive wear mechanism, adapted from [102]

Abrasive wear occurs when asperities of a rough, hard surface or hard particles are embedded in one or both of the mating surfaces in relative motion. These hard particles may be the product of processing, wear debris or dirt from outside of the tribo-system, Figure 3.6.

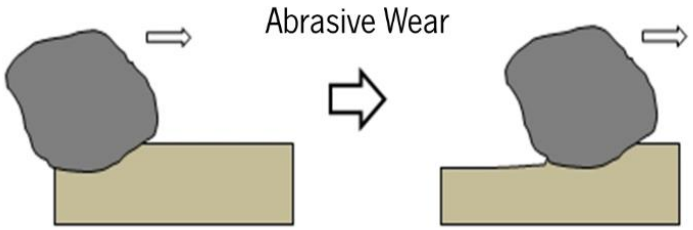

Figure 3.6: Representation of abrasive wear mechanism, adapted from [102]

The abrasion mechanism may be due to the penetration of the asperities of the hard material in the soft material (two-body abrasion) or due to small hard particles present at contact

interface, that are able to abrade either one or both of the surfaces in contact (three-body abrasion) [94]. The volume of abrasion wear is given by the Equation 3.5:

$$V = K_{abr}\frac{Wx}{3\sigma} \tag{3.5}$$

Where V is the wear volume, K_{abr} the wear coefficient by abrasion, W the normal load; x the distance of sliding and σ is the yield stress of the softer material. K_{abr} depends on the roughness of the hard surface, which means that this type of wear can be reduced improving the surface quality of the harder surface. The three-body abrasion mode reveals typical values for K_{abr} one order of magnitude lower than two-body abrasion mode. Once, many particles tend to roll rather than slide, as the abrasive particles spend about 90% of the time rolling, and the remaining time in sliding and abrading the surfaces [94,99,109].

Fatigue wear is related to the repeated loading and unloading cycles to which the materials are exposed. This may induce the formation of subsurface or surface cracks, which can result in the breakup of the surface with the formation of large fragments, leaving large pits on the surface. The fatigue of materials may be manifested by the occurrence of elastic and plastic deformation, hardening, or softening the material and appearance of cracks and their propagation [99,101].

However, cracks can still be initiated from the surface by the mechanical and chemical interaction between contacting surfaces and surrounding environment or the interfacial element shown in Figure 3.7.

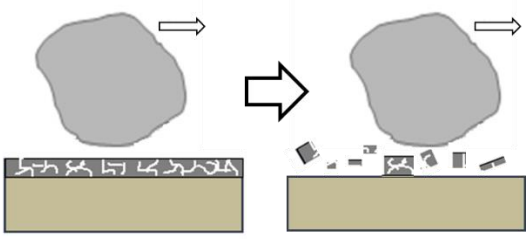

Figure 3.7: Representation of fatigue wear due cyclically applied loads, adapted from [102]

The surface fatigue may also be associated with mechanisms of adhesion or abrasion since the repetitive sliding of hard asperities on a solid surface can lead to the formation and propagation of cracks on the surface or subsurface. Other modes of wear that can occur in some

components and under some conditions are impact by erosion or percussion, chemical wear, such as corrosion, and electrical-arc-induced wear [102,112].

The wear of a mechanical component can be measured by its weight loss, due to an irreversible deformation or by the variation of surface roughness. Tribological tests allow to characterize the friction and wear behavior of materials in sliding contact in the absence or presence of a lubricant [94,99,100].

In order to minimize or control wear and friction at the contact surfaces, a protective film or a fluid between surfaces in sliding or rolling contact is required, **lubrication** is then an efficient method proved for this purpose. Lubricants also perform other functions, such as carrying heat and contaminants away from the interface. Thus, the reduction of friction between the bodies in contact also promotes a decrease in the wear of surfaces and reduces the heat generated between the surfaces [94,112]. They are often liquids, but there are some applications where lubricants can be gases or even solids. Depending on the thickness of the lubricant film, various regimes of lubrication may be defined. Although the friction in lubricated interfaces is typically less than that without a lubricant, there is still friction, and the magnitude of that friction depends on the fluid viscosity and operating conditions [94,100,112]. The effects of relative speed, load, and viscosity on friction are described by the Stribeck curve shown in figure 3.8.

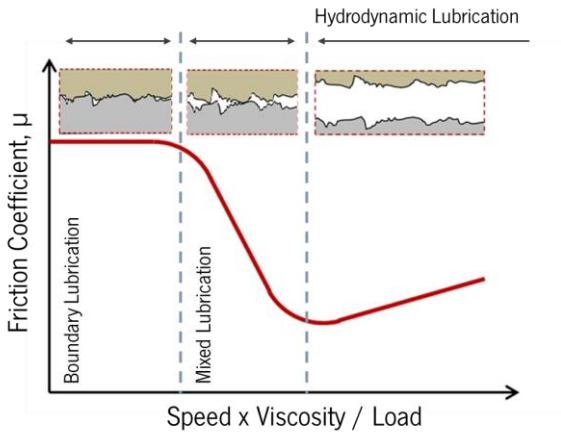

Figure 3.8: Variation of coefficient of friction with the specific film thickness, adapted from [102]

In boundary lubrication solid surfaces are so close to each other, with significant asperity interaction, this regime of lubrication is comparable to the non-lubrication conditions at the contact area, once the presence of lubricant film between the surfaces is very small, in the range 0.005-0.1 μm. In the case of hydrodynamic lubrication regime, the two surfaces are completely separated

by a lubricant film, with a considerable thickness between 1 and 100 μm or more. Once the hydrodynamic pressure is low compared to the strength properties of the solids, this will not cause appreciable plastic deformation. The condition of hydrodynamic lubrication is governed by the bulk physical properties of the lubricant, mainly by the viscosity [94,113,114].

The mixed lubrication regime corresponds to the transition between the boundary lubrication and hydrodynamic lubrication. The surfaces are mostly separated by a thin lubricant film although asperity contact still takes place. The total applied load is thought to be partly supported by asperity contacts and hydrodynamic action. Mixed lubrication has been defined with a lubricant film thickness ranging from 0.01 up to 1 μm. Another lubrication regime is the elastohydrodynamic lubrication, where the local elastic deformation of the solids provides a coherent hydrodynamic film, which prevents asperity interaction. The combination of the sliding speed, elastic deformation and the increase in lubricant viscosity allow the formation of a film with sufficient thickness to separate the two contact surfaces[109,112,113].

3.3 Biotribology in the Oral Cavity

In the history of humankind, wear of human teeth was always present and regarded as physiological. Teeth that were found in human skulls, dated back as early as 160,000 years ago, were so heavily worn that they did not demonstrate any anatomical tooth morphology. The extent of wear was mostly related to nutritional habits, which changed over time [115].

Also, the oral environment plays a very important role in the tribological behavior of human and artificial teeth. Dental wear, might either be a natural or artificial phenomenon, usually is the combination of chemical, biological and behavioral factors. Therefore, this is an environment auspicious to tooth structure degradation, being possible to identify several tribological phenomena [4].

Wear of teeth mainly results from mastication process; the action of chewing food involves an open and a closed phase. The open phase doesn't involve any occlusal forces where none or very little tooth wear occurs, on the other hand, in the closed phase, occlusal loads are applied and hard particles in foods are dragged across opposing surfaces, causing occlusal surface wear. It is possible to relate the wear volume resulting from food particles with normal applied load, which was found to progressively increases with the increase of applied forces [20,116].

Regarding behavioral phenomena, pathologies as thegosis and bruxism also can cause extreme tooth wear. Thegosis can be defined as the action of sliding teeth into lateral positions, which is considered a genetically determined habit to sharpen teeth. And bruxism, associated with a response to stress, is the action of grinding teeth without the presence of food. During these pathological actions, high occlusal forces are applied and, due to the direct contact between dental surfaces and the associated friction, tooth wear occurs, giving rise to loss to the vertical height of the tooth or dental restoration, which will have an impact on occlusal movement and constrictions in the temporomandibular junction, as well as hinder chewing. The results of bruxism can be seen in Figure 3.9 [11,20].

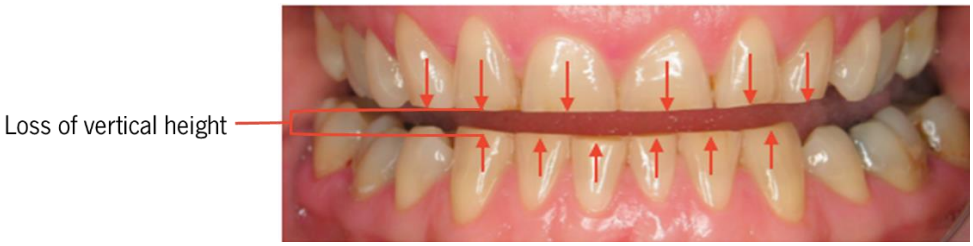

Figure 3.9: Vertical loss of dental height in patient suffering from bruxism [117]

Besides, nowadays, chemical effects play an increasingly significant role in tooth wear, mainly due to the large consumption of acid drinks. Additionally, tooth wear can also result from tooth cleanings such as tooth-brushing and habits such as pipe smoking and pencil chewing. The relationship of movement and tooth wear is shown in Figure 3.10 [20,118–120].

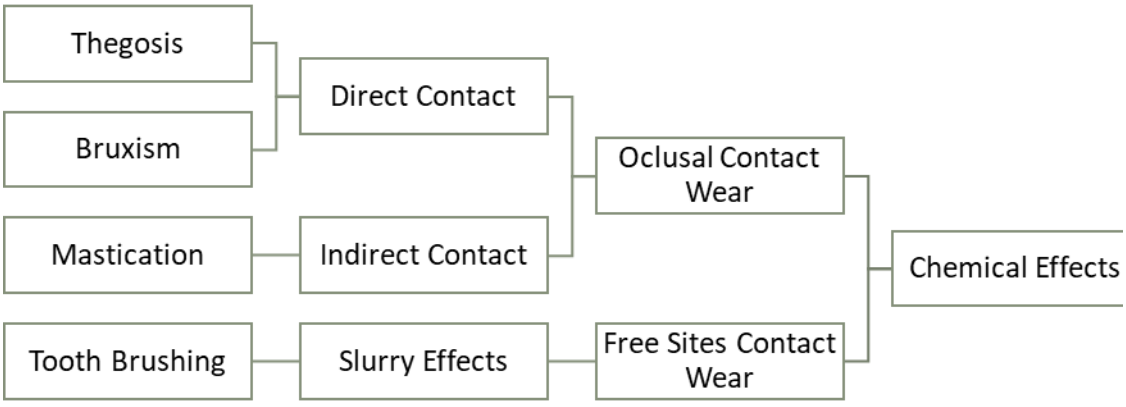

Figure 3.10: Relation between movement and wear of teeth, diagram adapted from [11]

From a scientific standpoint, people only started to pay attention to friction and dental wear mechanisms in the 18th century. John Hunter in 1771, described in one of the first textbooks in

dentistry “The Natural History of Human Teeth: Explaining Their Structure, Use, Formation, Growth, and Diseases”, three modes of tooth wear: abrasion, attrition, and erosion [30].

The three terms, attrition, abrasion and erosion are used in dentistry to describe dental and dental materials wear. These concepts are quite different from the tribological terms used in engineering to describe similar wear processes [121].

Abrasion, wear mechanism at non-contacting sites which cannot be ascribed to erosion or attrition. Consists in the friction between the tooth or restoration and an exogenous agent, causing one form of wear, that normally is the result of the three-body interaction, shown in Figure 3.11 (A)(B) regarding mastication. This mechanism may be of artificial origin, where the tissue loss occurs in a non-natural mechanical process, such as brushing the teeth, shown in Figure 3.11 (D) showing the tooth-brushing process. The benefits of tooth brushing are greater than the disadvantages, and tooth-brushing alone has no effect on enamel and very little on dentine, but too aggressive brushing, the use of abrasive toothpaste, and improper use of dental floss can lead to abrasion damage [122,123].

Accordingly, professional recommendations for individual oral hygiene mostly include tooth brushing at least twice daily for 2—3 min, with gentle force as suggested by the American Dental Association. Yet, ‘‘gentle force’’ is not defined clearly enough to be used in the clinical situation, and can be interpreted differently from individual to individual [124–126].

Previous studies have reported brushing forces ranging from 2.3 N to 3.23 N and even 11.3 N, variations associated with the gender, age, dental characteristics and measuring system [124,127,128]. Other experimental studies indicate that, in order to prevent a gingival recession, the brushing force should not exceed 3 N [129].

In Vivo studies, comparing the brushing forces applied with manual and sonic toothbrushes, the average brushing force of manual toothbrushes (1.6 N) was higher than for sonic toothbrushes (0.9 N) [130].

Physiological abrasion occurs when there is a natural loss of dental tissue and prophylactic abrasion results from the action of pathogens [121]. The researcher Peter Heaseman, found that plaque removal is improved with longer brushing time up to two minutes and with greater pressure up to 150 grams of pressure, that correspond to 1.47 N. More recently, the same researcher

tested 16 different ways of brushing teeth, and found that people in their daily life tend to brush their teeth for approximately 30 seconds and with a load close to 0.74 N [131,132].

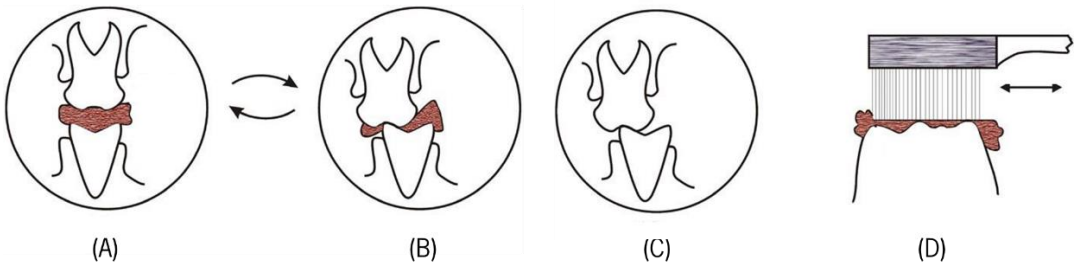

Figure 3.11: Schematic representation of the interaction between dental surfaces contact. (A) representation of mastication – open phase; (B) representation of mastication – closed phase; (C) direct contact between tooth structures; (D) tooth brushing; [4].

Attrition, this mechanism, which describes the physiological wear of dental hard tissue as a result of direct contact among teeth and any other abrasive particles, are the result of the two-body interaction. This type of dental wear, is especially critical in bruxism patients, and is also illustrated in Figure 3.11 (C).

Zhou, studied the sliding friction and wear behavior of enamel and dentine against titanium spheres, using as a lubricant, artificial saliva [11]. The results show that the enamel region exhibits a smaller friction coefficient and better wear resistance compared with dentine region for the same tooth [4].

The tribological properties of human teeth were considered mainly dependent on their age. Comparing permanent with primary teeth, the permanent teeth at young and middle ages exhibited better wear-resistance. However, when permanent teeth at old age stage were considered, the wear-resistance was reduced [133].

Also, higher water content could reduce the value and fluctuation of the friction force on enamel surface and protect the surface from wear damage. Both occlusal conditions (such as occlusal surface roughness and load) and the properties of food particles (such as texture and size) could influence the wear rate of teeth [11,134].

Erosion, describe the surface loss attributed to chemical effects. Saliva has been considered a very important biological factor in the case of dental wear, namely in erosion mechanisms. Several salivary defensive mechanisms act during the erosive process, mechanisms that slow down the rate of enamel dissolution. Erosion can then, be related to the low salivary flow

and low protecting capacity. So, the protective properties of saliva are extremely significant for minimizing the corrosive effects of acids on teeth and restorations. Also, saliva can operate has lubrication for the oral environment, protecting the tooth during mastication [4,119,135,136].

Also mentioned in the technical literature are **Demastication** (chewing abrasive substances as chewing gum), **Abfraction** (wear near the gum line, followed by trauma) and **Resorption** caused by processes of biological degradation of substances produced by the body (demineralization). These mechanisms affect the teeth and lead to an irreversible loss of tooth structure from the external surface. All these mechanisms are present during normal oral functions and for that reason, wear is a cumulative, irreversible and multifactorial process. This phenomenon is also associated with factors like age, gender, alimentation, gastrointestinal disorders, environmental factors, congenital anomalies on the tooth tissue, and others [4,137–139].

Considering the complexity of the oral environment and its biomechanics, the wear mechanisms in artificial dental materials are usually complicated and include the same tribological phenomena named before. Mechanisms of attrition, abrasion, erosion and abfraction or fatigue, cause the loss of surface material of dental restorations present in the mouth [4,140].

Wear has been shown to be a major problem in the use of new restoration materials, and it is a parameter to be considered when developing new dental material. Particularly, when the materials under consideration are composite, once a low wear resistance of a material can lead to premature failure and restoration replacement. In other words, and considering studies made by Arsecularatne and Hoffman, in which is concluded that the wear behavior of enamel was ceramic-like to some degree, pointing to the fracture under elastic contact that is responsible for enamel wear [133], and that crack formation occurred near the wear scar subsurface [141]; it's important to understand the wear behavior of the dental material, to ensure clinical, and aesthetical longevity of the restoration. Recently, biotribological studies are focused on the wear resistance of artificial dental materials and the predisposition of these materials to create wear on the antagonist surfaces, especially against the enamel. Such as mentioned previously, in Chapter 2, the main problem when using composite materials is to ensure the necessary mechanical and tribological resistance, particularly when using these applied materials to posterior restorations, due to higher applied loads in this region, during mastication, that sometimes results in the loss of anatomical shape of the restorations [4,5].

Taking all these into consideration, there is no doubt that human teeth are a superior natural tribological system. In fact, many tribological systems in engineering are more or less similar to the human teeth system with regard to friction and wear. With the developments in materials science and surface technology, the wear resistance of engineering systems has been considerably advanced. Thus, more emphasis should be given to the knowledge of dental tribology and anti-wear properties, which may help to design optimized systems with longer lifespan [11].

4. MATERIALS AND METHODS

4.1 Materials

4.1.1 VITA Suprinity®

VITA Suprinity®, VS material in this study, from Vita Zahnfabrick, also reflects the progress in this field, Figure 4.1.

Figure 4.1: VITA Suprinity® (VS) block for CAD/CAM processing [65].

This material derivates from the development of zirconia dental restorations, that allowed, for the first time, the fabrication of multiunit, all-ceramic bridges, and lithium disilicate ceramic, that presented high strength and a tooth-colored appearance. In Table 4.1, is possible to see the overall composition of this reinforced glass-ceramic [140,141].

Table 4.1: Chemical composition of the ZLS glass-ceramic [142].

Components	SiO_2	Li_2O	ZrO_2	P_2O_5	K_2O	Al_2O_3	CeO_2	Pigments
%Wt.	64 - 56	21 - 15	8 -12	3 - 8	4 - 1	4 - 1	4 - 0	6 - 0

The Zirconia reinforced Lithium Silicate (ZLS) glass ceramic, VS, shows a homogeneous structure in its fully crystallized form. The crystalline structure consists of small size crystal, approx. 0.5µm, almost three times smaller than lithium disilicate crystal phase. The overall composition of VS ensures that this material is capable of withstanding high loads, promise to enhance the durability by preventing catastrophic fracture of the restoration. As seen in Table 4.2, the material respects the requirements of ISO 6872 [142,143].

Table 4.2: Physical properties of the ZLS glass-ceramic [142].

Test	Experimental values	Standard values
Flexural strength (MPa)	≈ 420	> 100
Biaxial strength (MPa)	≈ 540	> 100
Modulus of elasticity (GPa)	≈ 70	None specified
Chemical solubility (µg/cm^2)	≈ 40	< 100

VS material presents a fracture toughness (K_{IC}) of 2.0 MPa.m$^{1/2}$, that is equivalent to more than four to five times the loads applied during the mastication cycles, which shows that the reinforcement is favorable to the prevention of premature failure of the restoration due to applied loads [142].

On the other hand, its elasticity modulus is lower than the occlusal enamel, which can cause plastic deformation of the restoration. Given that its hardness is roughly 7 GPa, which is higher than higher human teeth, it can promote the wear of the natural antagonists [144,145].

VS material presents good mechanical and physical properties, alongside with high translucency, fluorescence, and opalescence. All these characteristics led to an increase of interest for this material by the dental community. However, as the VS material is only on the market since a few years ago, their tribological properties are still poorly unknown, making it important to characterize the friction and wear behavior [142,145].

4.1.2 VITA Enamic®

The newly developed polymer infiltrated ceramic network, VITA Enamic®, VE material in this work, also from Vita Zahnfabrick, may offer an alternative solution. It has a lower tendency to brittle fracture than pure ceramics, and excellent CAD/CAM processing [90].

Figure 4.2: VITA Enamic (VE) block for CAD/CAM processing [90].

This hybrid material is composed of a ceramic porous matrix, in which the pores are filled with a polymer material, in a mass percentage of 86%wt., for the inorganic ceramic part, and 14%wt. of organic polymer part. The chemical composition can be seen in Table 4.3.

Table 4.3: Chemical composition of the VE [90].

Composition	Inorganic part (86%Wt.)					Organic part	
Chemical compounds	SiO_2	Al_2O_3	Na_2O	K_2O	B_2O_3	UDMA	TEGDMA
%Wt.	55 - 50	19 -17	9 - 7	5 - 3	2 - 0.5	14	

The composition of the ceramic corresponds to that of a fine-structure feldspar ceramic enriched with aluminum oxide. This material, by itself, is not known for having the best mechanical properties, but with the introduction of the urethane dimethacrylate (UDMA) and triethylene glycol dimethacrylate (TEGDMA), its physical and mechanical responses have been improved, meeting the requirements of ISO 6872 and ISO 10477, shown in Table 4.4 [143,146].

Table 4.4: Mechanical and physical properties [90,143,146].

Test	Experimental values	Standard values
Flexural strength (MPa)	150 – 160	>50[a] and > 100[b]
Modulus of elasticity (GPa)	30	None Specified
Chemical solubility (μg/cm^2)	0.0	< 100 [a]
Water absorption (μg/mm^3)	5.7	< 40 [a]

[a] Values referent to ISO 10477; [b] Values referent to ISO 6872.

With a fracture toughness of approximately 2.3 MPa.m$^{1/2}$, slightly higher than the reinforced glass ceramic, VS, the VE dental material is less fragile and has less tendency to catastrophic fracture. However, this material possesses a much lower modulus of elasticity and hardness than enamel, which can compromise the integrity of the restoration when inserted into the oral cavity.

Also, there is few information regarding the *in vivo* success of this restoration material, neither in detail studies regarding VE or other polymer infiltrated ceramic dental materials.

4.2 Sample Preparation

Samples of ZLS glass ceramic (VITA Suprinity, Vita Zahnfabrik, Germany) and polymer-infiltrated composite samples (VITA Enamic, Vita Zahnfabrik Germany) were cut from standard blocks for CAD/CAM. Samples were obtained from slices with 3 mm thickness and 10x10 mm cross-sectioned area for tribological tests. The cut process was performed using a 0.5 mm diamond disc coupled to a cutting machine (Struers Miniton, USA) presented in Figure 4.3.

Figure 4.3: Cutting equipment, *Struers Miniton*

After the cutting process, all the samples were polished using silicon carbide abrasive grinding paper (180 - 2000 grit), to reach a roughness below 0.1 µm [147]. This process was followed by ultrasonically cleaning with isopropyl alcohol for 10 min.

In order to ensure that the surface roughness was within the parameters, the average roughness (R_a) of all samples was measured using a profilometer (*Surfest*® SJ-210, Mitutoyo America, Japan). VS showed a R_a roughness at 0.036±0.002 µm while VE samples revealed a R_a roughness at 0.053±0.006 µm.

4.3 Linear Reciprocating Sliding Tests

The sliding tests were performed on a reciprocating sliding tribometer (Plint TE 67-R, England), operating in ball-on-plate geometry, as shown in Figure 4.4.

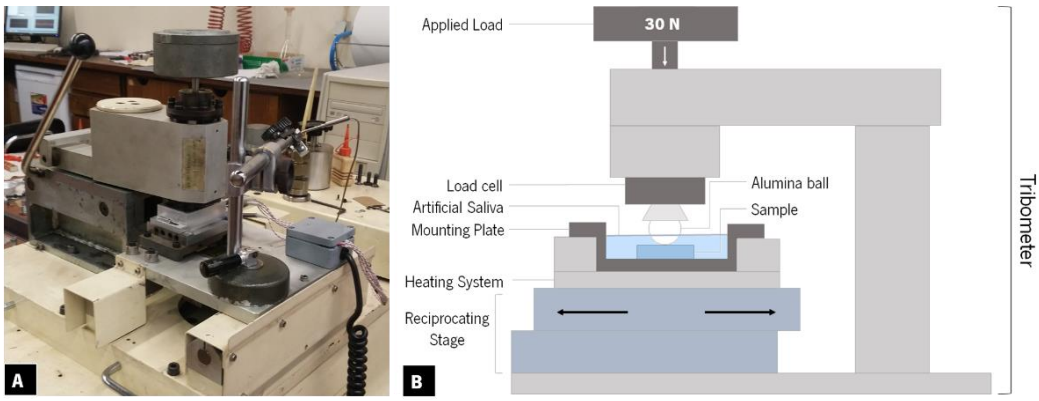

Figure 4.4: (A) Reciprocating sliding tribometer (Plint TE 67-R); (B) schematic representation of the tribometer and test set up.

Before testing, the samples were ultrasonically cleaned immersed in isopropyl alcohol for 10 minutes. An alumina ball with 10 mm diameter was used as counter body. The sliding tests were carried out in Fusayama's artificial saliva as described in Table 4.5. The solution maintained at 37 ±1 °C to mimic the temperature in the oral cavity. These parameters meet the tribological test models previously reported, as illustrated in Figure 4.4 (B) [148].

Figure 4.5: *Fusayama* artificial saliva composition [148].

Components	Ureia	$CaCl_2.2H_2O$	$NaH_2PO_4.2H_2O$	NaCl	KCl	$Na_2S.9H_2O$
g/L	1	0.795	0.69	0.4	0.4	0.005

The procedure of wear testing followed a rate of 60 cycle/min on 30 N loading for 1 h or 2 h. A process similar to the one followed by Imai et al. [149], Coppedê et al. [149] and Faria et al.,[150]. These conditions represented the wear of dental materials, for 60000 cycles, which is approximately similar to 120 days of mastication. To ensure the reproducibility of results, three independent experiments were run per test condition.

Figure 4.6: Detail of the mounting plate and one of the samples of the composite material

The antagonist material chosen was alumina, since this material is tribologically well-characterized. During the sliding tests, the coefficient of friction (COF) was continuously recorded using the specific computer program associated to the tribometer. Then, different segments of COF plots were studied, to obtain the steady-state friction coefficient, for each material against alumina.

As a result of the sliding cycles, wear grooves are formed on the surface of the flat samples under study. Such grooves are named wear tracks as shown in Fig. 4.7. The wear volume can be evaluated from the measurements of the wear track caused by the penetration of the alumina ball on the test samples.

After the reciprocating sliding tests, the wear volume was estimated by measuring the

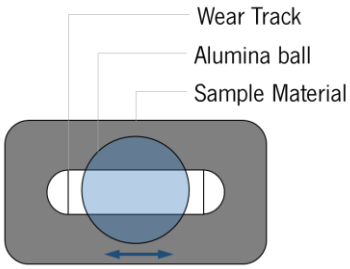

Figure 4.7: Schematic representation of the wear track formation, diagram adapted from [151].

lateral width, on three different points of the wear tracks. The volume loss values of the samples were determined by following the wear track model represented in Figure 4.8.

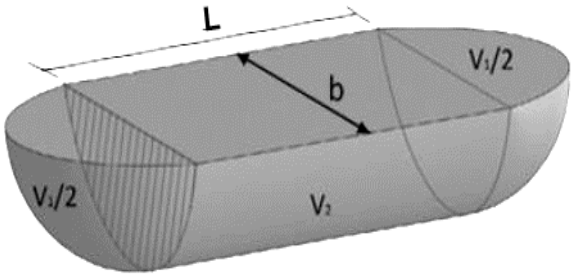

Figure 4.8: Wear track model, adapted from [152].

Assuming that the wear tracks are formed by a perfect ball geometry, the volume of wear can be calculated by empirical mathematical equations. At first, the mid zone area of the wear track must be estimated. The calculation was then performed accordingly to the schematic representation in Figure 4.9. The total volume loss of the wear track corresponding to the wear of the flat samples was calculated using the Equation 4.1:

$$\Delta V = L \times \left[\frac{1}{2} \times R^2 \times 2\sin^{-1}\left(\frac{s}{R}\right) - \frac{b \times h'}{2}\right] + \frac{\pi \times h'}{64R} \qquad (4.1)$$

where, ΔV is the total volume loss of the wear track, in mm^3, L is the stroke length in mm, R is the radius of the alumina ball in mm, s is the half of the width of the wear track (s=b/2) in mm and h' is the height of the triangle in mm, as shown on the Figure 4.9 [152,153].

The volume loss values were then converted into specific wear rate using the Equation 4.2, where

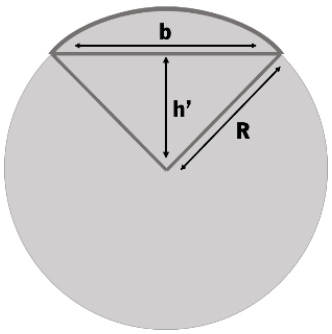

Figure 4.9: Diagram of the calculations for the area of the mid-zone of the wear track [152].

k is the specific wear rate in mm^3/N.m, and W the applied load in N, and S the total sliding distance in m [152,153].

$$k = \frac{\Delta V}{W \times S} \tag{4.2}$$

4.4 Micro-Scale Abrasion Test

Micro-scale abrasion tests were performed using a TE-66 micro-scale abrasion equipment (Phoenix Tribology Ltd, UK) schematically shown in Figure 4.10.

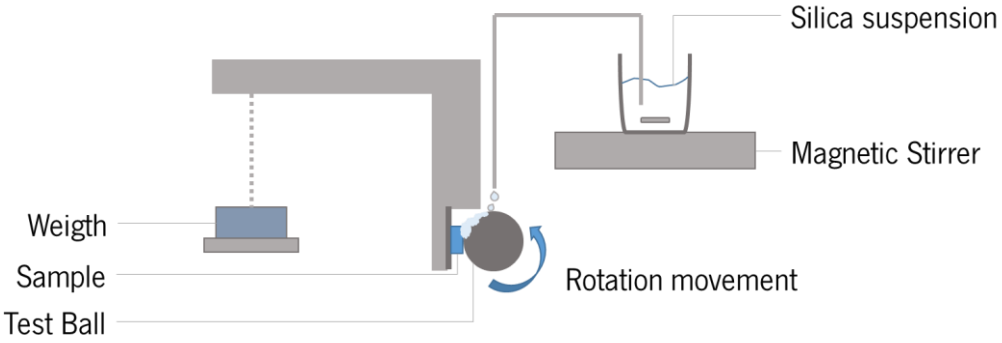

Figure 4.10: Schematic representation of the micro-scale abrasion test

The samples were mounted on an aluminum plate which was then attached to the micro-scale abrasion machine. The abrasive slurry was prepared by dilution of 8-10 µm hydrated silica (*Tixosil* 73, *Solvay*) in distilled water with a proportion of 1/16 (%wt.). This abrasive suspension was maintained homogenized during the tests using a magnetic stirrer and tests identified as C 1/16. Tests were also performed in distilled water, i.e. without any abrasive particle to be considered as a control group (C0).

The micro-scale abrasion tests were performed against a stainless-steel ball (ASTM 52 100) with 25 mm diameter rotating at 60 rpm for 600 revolutions. All the tests were performed at 0.8 N normal load. Three experiments were performed per test condition for each material sample. Before and after the experiments, the samples were ultrasonically cleaned with isopropyl alcohol for 10 min, and stored for later surface characterization.

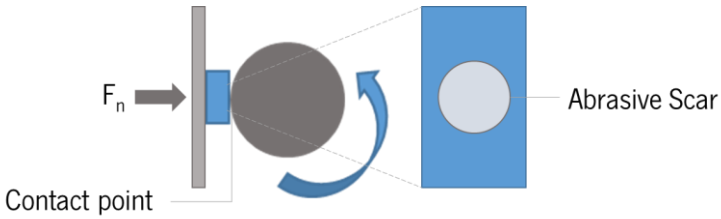

Figure 4.11: Schematic representation of the results of micro-scale abrasion tests, adapted from [151].

The volume loss of tested samples was estimated based on the wear scar diameter measurements and assuming that the morphology of the wear scars was similar to the shape of the test ball, as represented in Figure 4.11. Therefore, the volume loss can be calculated using Equation 4.3 [151,152].

$$\Delta V = \frac{\pi \times c^4}{64R} \tag{4.3}$$

Where ΔV is the crater volume, c is the crater diameter and R is the radius of the test ball where b<<R. The diameter of each wear scar was measured by scanning electron microscopy and using the *KLONK* image measurement software.

4.5 Microstructural Characterization

After the tribological tests, samples were ultrasonically cleaned using the same procedure previously described. All the worn surfaces were inspected by Field Emission Gun Scanning Electron Microscopy (FEGSEM, JSM-6010 LV, JEOL, Japan). The chemical composition of the ZLS and Enamic surfaces and tribo-layers were inspected before and after the wear tests by Energy Dispersive Spectroscopy (EDS) (INCAx-Act, PentaFET Precision, Oxford Instruments), in order to confirm the chemical nature of the formed adherent tribo-layers, during the tribological tests. This equipment is shown in Figure 4.12.

Figure 4.12: Field Emission Gun Scanning Electron Microscope (FEGSEM) with an Energy Dispersive Spectroscope (EDS)

VS and VE samples were previously sputter-coated with Gold-Palladium in order to make the surfaces conductive, obtaining a higher resolution in the micrographs, and thus allowing the acquisition of quality images with greater magnifications for FEG analyses. For each wear track and abrasion scar, images were acquired with magnification ranging from x40 up to x2000.

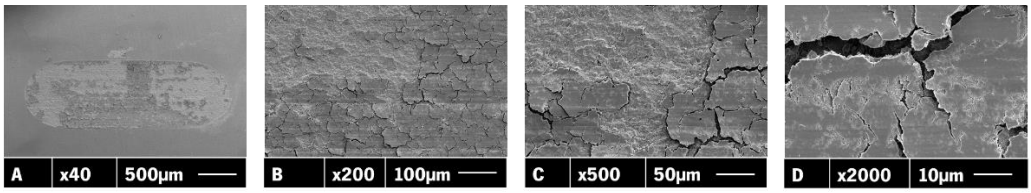

Figure 4.13: Group of SEM images for different magnifications. (A) general appearance of a sliding wear track (40×); (B) and C intermediate magnifications (200× and 500×) (D) detail view of the sliding wear track (2000×)

EDS analysis was also performed (*INCAx-Act*, *PentaFET Precision*, *Oxford Instruments*), to analyze the composition of the VS and VE surfaces, before and after the wear tests, in order to confirm the nature of the adherent tribo-layers formed during the tribological tests.

5. RESULTS AND DISCUSSION

5.1. Linear Reciprocating Sliding Test

A set of tribological tests involving reciprocating sliding of the two materials in study (VS and VE) against an alumina ball were performed in Fusayama's artificial saliva at 37 °C. All the sliding experiments were conducted with a fixed normal applied load of 30 N, stroke length of 2 mm, and an oscillation frequency of 1 Hz for 3600 s and 7200 s. The variation of sliding times, was made primarily to ensure the stabilization of the coefficient of friction (COF) for both materials, and posteriorly to perform a detailed analysis of the wear mechanisms of the VE/alumina pair.

5.1.1. Frictional Behavior

The evolution of COF for material VS against Al_2O_3 in presence of artificial saliva during the 2 h test is shown in Figure 5.1. The shape of the COF plot is quite representative of the friction against alumina for 1 h sliding.

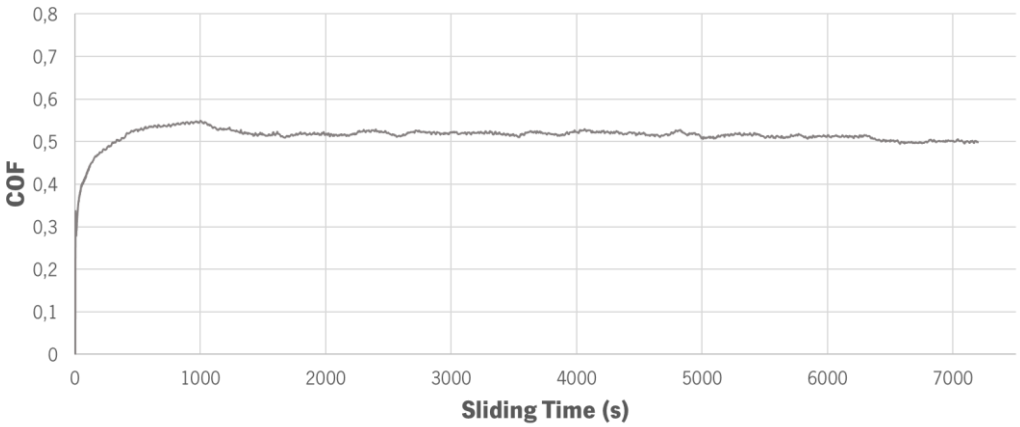

Figure 5.1: Evolution of the coefficient of friction (COF) with time for VS against Al_2O_3 in Fusayama's artificial saliva at 37 °C (F_N = 30 N, stroke length 2 mm, 1 Hz, 2h of sliding).

As seen in Figure 5.1, a running-in period takes places at a maximum COF values at around 0.54 for 1000 s followed by a steady-state regime in which COF stabilizes around 0.52. The small oscillations noticed on the COF values during the steady-state regime can be explained by the formation of periodic localized fractures, and possible adhesion phenomena that can occur between the bearing surfaces. On the other hand, the formation of third bodies at the contact interface due to the release of wear debris from of the VS material, can also contribute to the small fluctuations of COF values [97,102,107,109,153].

Arsecularatne et al. performed reciprocating sliding wear tests with leucite glass-ceramic against enamel. The results revealed that the dominant wear mechanism for the reinforced glass-ceramic was micro-abrasion due to lateral crack formation. Enamel presented signs of delamination due to the action of the hard asperities of the microstructure of the glass-ceramic material. This reinforced glass-ceramic present similar properties with the material VS, however the leucite glass-ceramic presented COF values rounding 0.21-0.25. Though, it is not possible to directly compare the values, since the tests conditions and antagonist surfaces were different. [154].

In the case of the VE samples, although subjected to the same testing conditions, the COF behavior was noticeable from the friction evolution curve obtained for the contacts involving VS samples. Instead of a relatively short running-in period, the COF response was characterized by a long period of sliding where the friction coefficient continuously increased, for an experiment corresponding to 1 h test. Due to this particular friction behavior revealed for tests involving VE

samples, it was decided to increase the sliding time up to 2 h, resulting in the frictional behavior shown in Figure 5.2 [102,155].

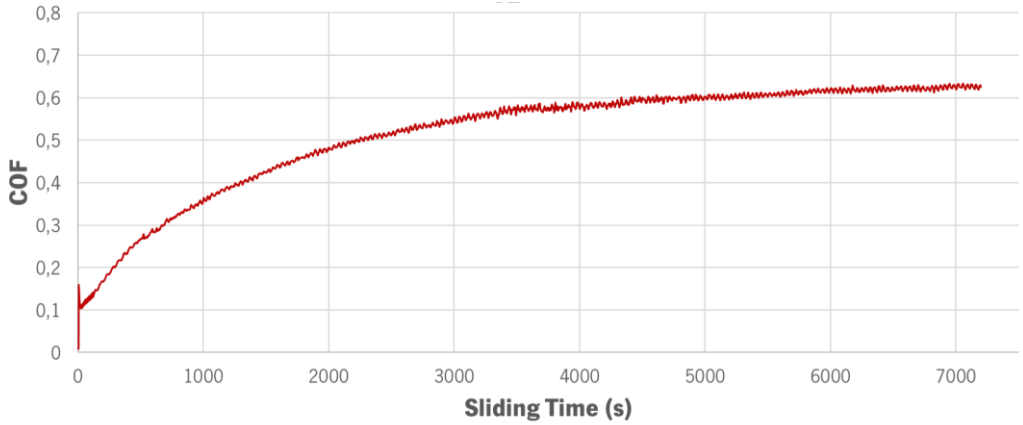

Figure 5.2: Evolution of the coefficient of friction (COF) with time for VE against Al_2O_3 in Fusayama's artificial saliva at 37 °C (F_N = 30 N, stroke length 2 mm, 1 Hz, 2h of sliding).

In Figure 5.2, it's noticed the progressive increase in friction force values after a small initial peak that occurs in the first 30 s of sliding. That peak in COF could be attributed to the fact that tests have been performed in the perpendicular direction to the polishing grooves. Hence, the peak can occur due to a period of adaptation of the alumina ball sliding to the rough surfaces. Subsequently, an abruptly drop in the COF was noticed although that was followed by an extensive running-in period characterized by progressive increasing in the friction force values over 6000 s. A steady-state regime in COF at 0.62 was detected from around 6000 up to 7000 s.

Comparing these values with the study carried out by Arsecularatne et al. who performed a reciprocating sliding test in three different resin composites and excluding the initial "run-in" stage, the average coefficient of friction values measured were in the range 0.03–0.09, with no significant variation depending on the composite or contact load. Which may indicate that the high COF value obtained for the VE samples, may be directly related with the polymer and ceramic interface [156].

COF curves of the three independent tests performed on different surface areas of the VE samples are shown in Figure 5.3. in the same sample surface. Due to this process, as seen in Figure 5.3, it was possible to verify the occurrence of large oscillations, after reaching the stabilization plateau, being more prominent for the last test (track C).

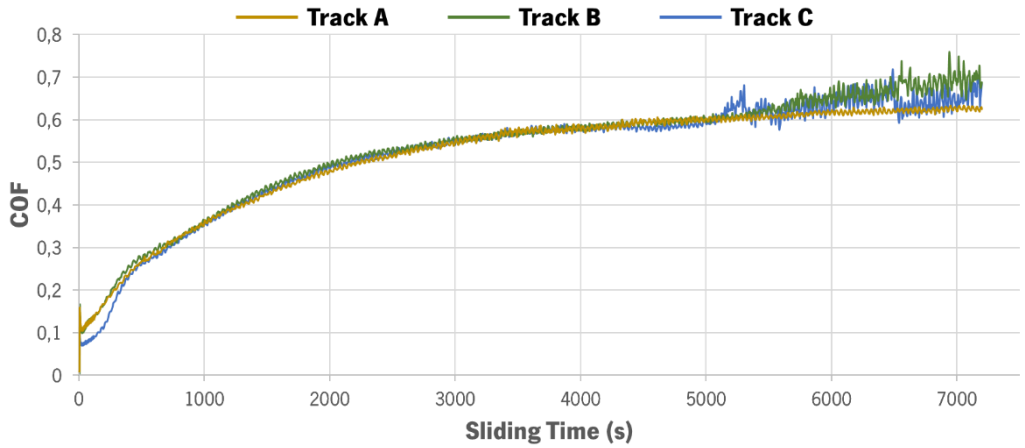

Figure 5.3: Evolution of the coefficient of friction (COF) with time recorded on VE samples against Al_2O_3 in Fusayama's artificial saliva at 37 °C (F_N = 30 N, stroke length 2 mm, 1 Hz, 2h of sliding), for three different and sequential wear tracks in the same sample.

The COF curve shape for the same VE sample tend to become unstable with the course of the sliding test repetitions. This phenomenon can be related with the immersion time of the samples in the artificial saliva. For the first test (track A), the sample was immersed in Fusayama's artificial saliva for 9600 s, corresponding to the test duration (7200 s) and tribometer heating period (2400 s). After this test the artificial saliva was changed, to prevent the accumulation of debris in suspension. After the second test (Track B), the sample was immersed over a period of 17000 s. At the end of the third test (Track C), the time of immersion of the sample reached 24000 s. Given the fact that the VE material has a reported water absorption mean value of 5.7 µg/mm^3, hydrolysis of the polymer can occur due to the water absorption leading to a more pronounced degradation of the contact surface and increased formation of debris , with effects on the fluctuations of friction values [90].

In addition, the oscillations in the COF values are usually associated with localized fracture of the contact surface as well as due to the formation of third bodies (debris) from the material degradation under wear [153].

Restorative materials including VS and VE can be in sliding contact against teeth enamel under mastication, being subject to tribological phenomena. Typical COF values recorded for teeth enamel against similar surfaces are around 0.10 - 0.42 in human saliva, depending on the number of cycles, as shown in the work of Roy et al. [157].

Accordingly, with the literature, the ideal restoration should have a wear resistance similar to that of enamel, to cause the least damage as possible to the antagonist natural structures. In

order to that, Zhou et al. [158], investigated the frictional behavior of VE against enamel and against a ceramic, in a ball-on-plate tribometer, during reciprocating sliding under a load of 20 N. It was found that the VE/enamel pair presented the highest COF value (approximately 0.75), while the pair ceramic/enamel COF stabilized faster in a value around 0.45. Zhou attributed this difference to the microstructure of material VE, considering the repercussion of the dual interpenetrating three-dimensional intersecting networks, in the fracture mechanisms and accumulation of debris due to the sliding motion.

Results of the present study revealed a different wear behavior for VE and VS samples. Being the friction coefficient upon stabilization for VE higher and progressively more unstable than for VS material.

5.1.2. Wear Behavior

Through SEM analysis of the contact surface of the samples it is possible to identify the wear mechanisms that occurred during the tests of reciprocating sliding. In the micrographs presented in this study, the sliding direction is always considered horizontal.

FEGSEM Images of the polished surfaces of both materials, VS and VE, are shown in Figure 5.4. The R_a roughness recorded for VS was of 0.036±0.002 μm while R_a roughness for VE was at around 0.053±0.006 μm, meeting the requirements of R_a<0.1 μm for surface roughness of dental materials [147].

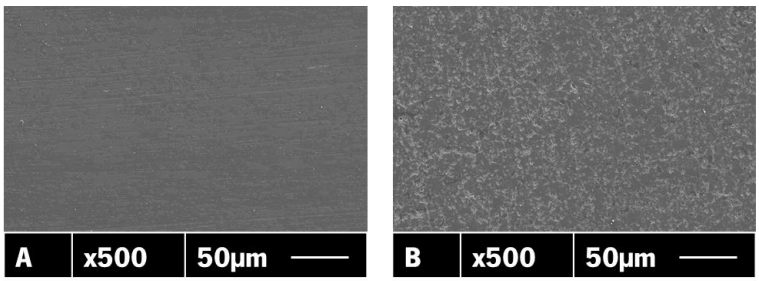

Figure 5.4: FEGSEM images recorded on polished surfaces of VS (A) and VE (B) samples.

The wear mechanisms of the test materials after reciprocating sliding can be evaluated by FEGSEM images in secondary electrons (SE) mode as seen in Figures 5.5-5.8.

Representative FEGSEM images of the wear tracks on the VS material are shown in Figure 5.5. Considering the morphological aspects of the wear tracks, the dominant wear mechanism is

characteristic of abrasion, as proved by the existence of grooves aligned according to the horizontal sliding direction.

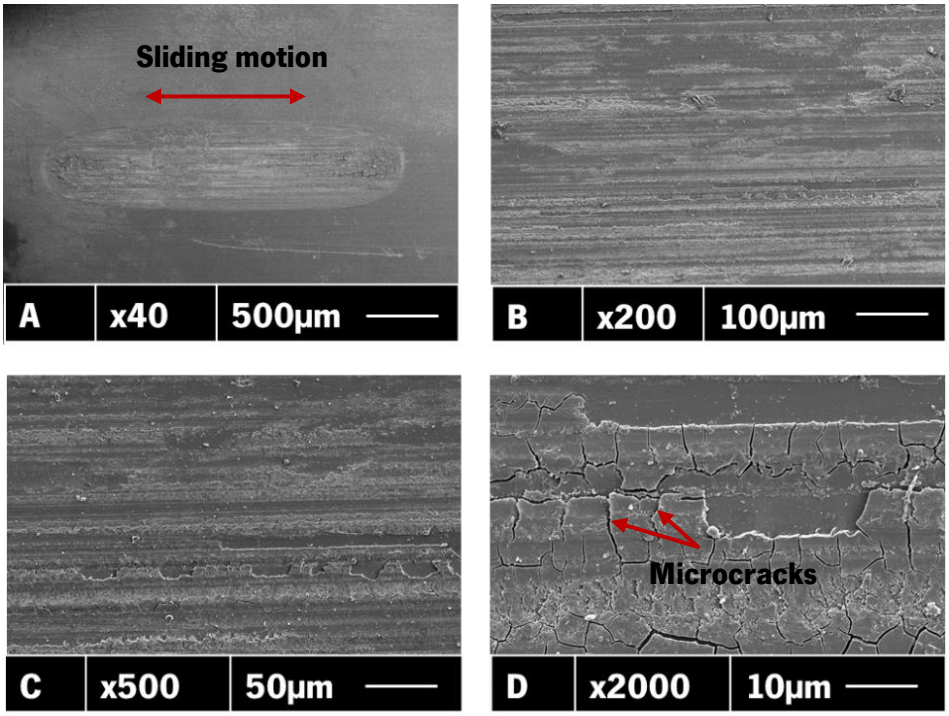

Figure 5.5: FEGSEM images of the worn surfaces of VS. (A) Overview of the wear track. (B,C) Sequential magnification of the middle region in the wear track the horizontal direction. (D) Detail of the sliding grooves (F_N = 30 N, stroke length 2 mm, 1 Hz, 2h of sliding)

At the edges of the wear track, it is noticed the occurrence of an adherent and thin tribo-layer is noticed, as the result of the adhesion of debris particles through the reciprocating sliding movement. This process tends to drag material, until eventually it disaggregate from the surface and, finally, promote the agglomeration of the adherent particles. It is also possible to notice the existence of relatively preserved zones alternating with abrasion grooves, such features are typical of ceramics and brittle materials [114,160].

Abrasion grooves were also detected on VE samples after a 1 h reciprocating sliding tribological test as shown in Figure 5.6.

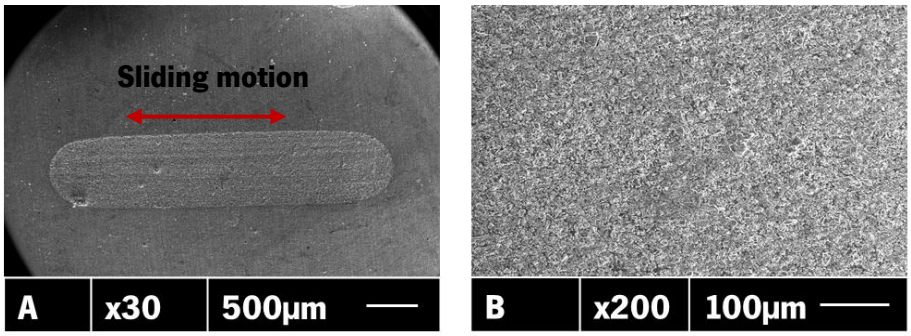

Figure 5.6: FEGSEM images of the VE worn surfaces. (A) Overview of the wear track. (B) Magnification of the middle region in the wear track (F_N = 30 N, stroke length 2 mm, 1 Hz, 1h of sliding)

The wear track on VE worn surfaces after 2 h sliding wear showed a different morphological aspect when compared to the worn surfaces after 1 h sliding, as shown in Figure 5.7. The formation of a thick and unstable tribo-layer dispersed along the length of the wear track was detected as shown in Figure 5.7(D). This tribo-layer is formed by the deposition of wear debris with aggregation of particles when immersed in artificial saliva [110].

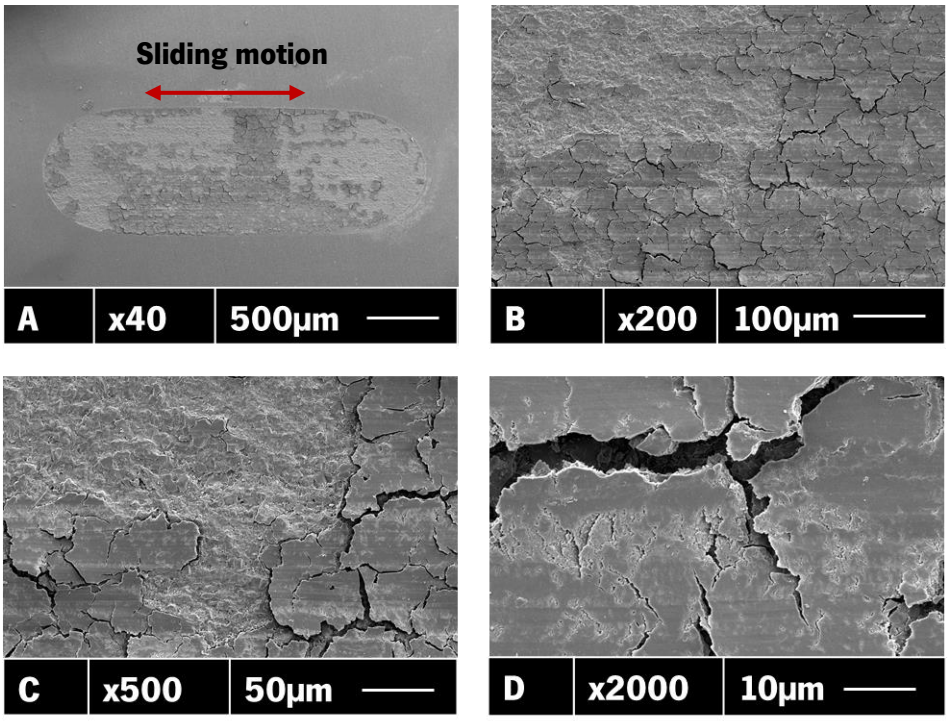

Figure 5.7: FEGSEM images of the VE worn surfaces: (A) Overview of the wear track. (B,C) Sequential magnification of the middle region of the wear track. (D) Detail of the tribo-layer (F_N = 30 N, stroke length 2 mm, 1 Hz, 2h of sliding)

Cracks can be noted in the wear track due to the fracture of the material surface during wear sliding movement (Fig. 5.7B-D). The process of cyclic loading on the tribo-layer promotes a successive removal of material., causing a "delaminated" zone to appear. This process is similar to what happens in pitting corrosion mechanisms. Particularly seen in Figure 5.7 (C), is that the fracture and removal of the tribo-layer exposes an irregular surface, thus increasing the roughness and contributing to the fluctuation in COF values during sliding (Figure 5.3).

Regarding the variation of the COF curves (Fig. 5.3) at the final period of the reciprocating sliding tests VE for 2h, the worn surfaces in the wear track middle region were carefully analyzed by FEGSEM. As shown in Figure 5.8, tribo-layers entirely coated the worn surfaces of the first wear track (A) revealing smaller micro-cracks when compared to the (B) second and (C) third wear tracks. Delamination of the tribo-layers are noticeable in the wear track C as a result of the progressive time of immersion of the test samples during sliding (Figure 5.3) In fact, the oscillation in COF mean values on Figure 5.3 can be linked to the accumulation of wear debris followed by formation and delamination of thick tribo-layers [159,160].

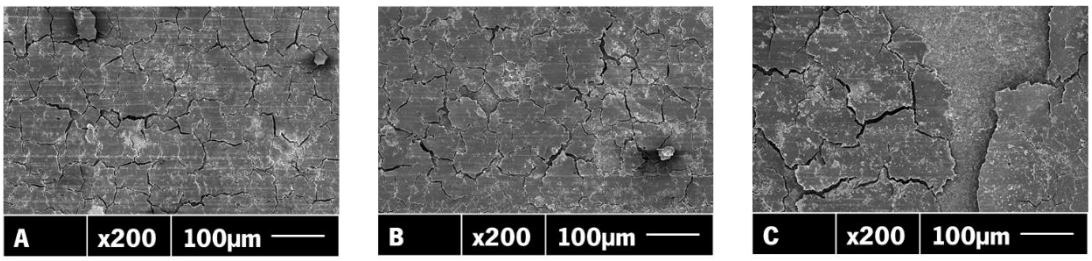

Figure 5.8: FEGSEM images of the worn surfaces of the sample of VE against Al_2O_3 in Fusayama's artificial saliva at 37 °C (F_N = 30 N, stroke length 2 mm, 1 Hz, 2h of sliding); (A) Track A; (B) Track B; (C) Track C.

Comparing SEM images of the wear tracks for 1 h, Figure 5.6 (B), and 2 h, Figure 5.7 (B), it was possible to verify that the surface on the 1hour worn surface, was much different than that obtained in 2hour tests. However, the new surface that appears after the delamination of the tribo-layer, is in all similar to the worn surface after 1h of test. Corroborating, with the presented theory, that the tribo-layer is composed by the aggregation of the debris particles [102,115,160].

In order to investigate the effect of the artificial saliva on the formation of the unstable tribo-layers, EDS analysis was performed in the wear track of the VE samples corresponding to 1 or 2 h sliding, which is shown in Figure 5.9.

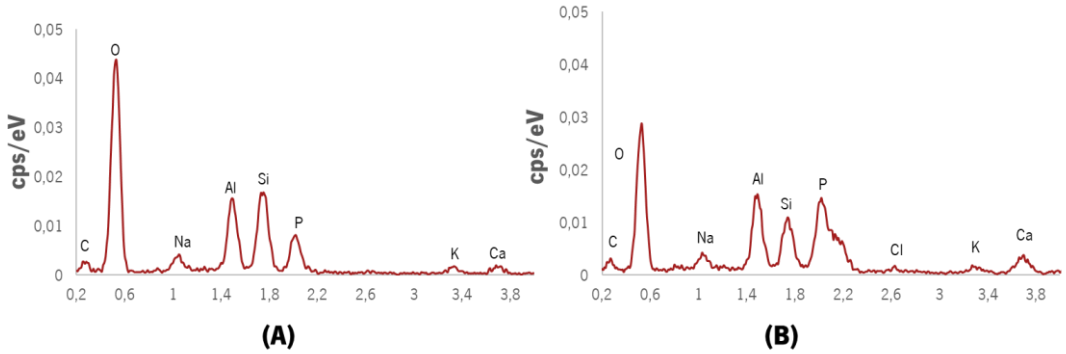

Figure 5.9: EDS plots for VE samples on the middle region of the wear track after reciprocating sliding tests against Al_2O_3 in Fusayama's artificial saliva at 37 °C (F_N = 30 N, stroke length 2 mm, 1 Hz); (A) 1h of sliding; (B) 2h of sliding (inside de region of the tribo-layer).

The chemical analysis performed on the tribo-layers in the wear track of the VE samples corresponding to 1 or 2 h sliding, some of these elements are contained in the artificial saliva solution, namely Cl, K, Ca and P, and were embedded in the tribo-layers (Figure 5.8 (B)). These results also corroborate with the previous assumption, that a chemical reaction between he VE material and the lubricating liquid occurs and promotes the agglomeration of the debris particles [100,161].

5.1.4. Wear volume

Mean values of the specific wear rate recorded for VE and VS samples after the linear reciprocating sliding tests are shown in Figure 5.10.

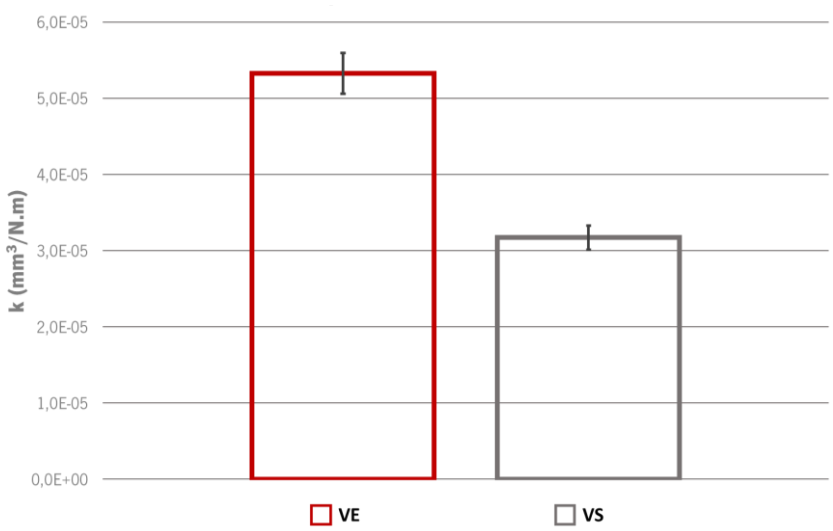

Figure 5.10: Mean values of the specific wear rate for material VE and VS, after reciprocating sliding tests against Al_2O_3 in Fusayama's artificial saliva at 37 °C (F_N = 30 N, stroke length 2 mm, 1 Hz, 2h of sliding).

As seen in Figure 5.10, a higher mean value of wear (k= 5.3x10^{-5} mm^3/N.m) was recorded for VE when compared to VS samples (k= 3.2x10^{-5} mm^3/N.m). These findings corroborate the COF results and the morphological aspects revealed by FEGSEM images. Mechanical properties such as elastic modulus, hardness and fracture toughness, play an important role on the wear volume of the materials. Considering the heterogeneous composition of the VE samples associated with the slightly higher R_a, different sections of the same sample might have different properties. These differences influence the friction behavior, contributing for a longer running-in period and instability of COF evolution.

Also, the thick and unstable tribo-layer presented in the micrographs of the wear scars of VE material during the sliding tests, presented more signs of a deeply worn surface, where the surface is irregular and full of microfractures. This can also be due to the organic part, and to the water absorption of the material.

Reinforcing the validity of the present results for the sliding tests, Mörmann et al. [162] reported that VE presents revealed higher wear resistance against human enamel, than other dental materials, with the exception of a zirconia-based ceramic. It was also concluded in the previous study, that VE has a wear behavior similar to that recorded for natural enamel, once both presented identical cracking and delamination defects. Similar results were later confirmed by Elhomiamy et al. [163], during tribological experiments performed on polymer-infiltrated and lithium disilicate glass-ceramics, against natural human enamel.

Stawarczyk et al. investigated wear simulating 5 years of mouth motion sliding contact of human enamel against various dental materials: resin composites, a polymeric infiltrated ceramic (VE), and a lithium disilicate glass-ceramic [164]. The VE samples showed less wear than the resin composites, and similar to glass-ceramics. Comparing the antagonist worn surfaces, the glass-ceramic showed to be more abrasive to enamel than the other two materials. A similar study made by Nathaniel et al. compared the tribological response of three different dental materials with a different methodology. Reciprocating sliding tests were done with resin composites, VE samples and a lithium disilicate glass-ceramic against human premolars, under glycerin lubrication. The wear was more prominent for the glass-ceramic than for the resin composites, the polymer infiltrated ceramic was the material with less wear volume loss and less wear caused on the opposing surface [164,165].

Another studied carried on by El Zhawi et al. that investigate the fatigue fracture resistance and wear behavior of VE samples, using a sliding-contact mouth-motion fatigue/wear test show that the failure was designated as chip-off or bulk fracture for all the specimens [166]. Comparing with the work of Swain et al. in similar conditions and in association with thermal cycling, that compared three materials, VE, feldspar porcelain and lithium disilicate. The VE samples survived the tests with minor wear, wheras feldspar ceramic crowns revealed significant fractures, and some of the lithium disilicate present minor cracking, for loads higher than 2000 N [166,167].

Taking all into account and opposing to what was observed in the present work, VE seems to have similar wear resistance to glass-ceramics, which are reported to yield acceptable antagonist enamel wear in vivo. On the other hand, the test conditions were quite different from those of the present study, hindering direct comparisons [164].

Dental restorations are simultaneously exposed to mechanical stress (e.g. mastication loads) and also exposed to the oral environment conditions (e.g. particles in suspension, pH, type of diet). This interaction can be responsible for the excessive wear of enamel and possible failure of dental restorations [24,40].

Manufacturing restorative ceramics by CAD/CAM is the most desired technique considering fitting and mechanical stability. However, the main problem is the brittleness and low fracture toughness characteristic of ceramic materials, which can lead to failure of dental restorations due to the propagation and catastrophic fracture of artificial crowns or dentures. [17,168].

5.2. Micro-Scale Abrasion Test

Micro-scale abrasion or ball cratering test is a technique for measuring the abrasion wear resistance of a surface of engineering components. This test consists in a mechanical system with a rotating ball on a flat test surface in the presence of a suspension containing abrasive particles. In this study, the rolling movement transporting the abrasive particles to the contact interface was promoted by a stainless-steel ball, against the flat samples of VS and VE materials, in the presence of a hydrated silica suspension of 1/16 %wt. From the generated wear scars the wear volume was measured and the wear mechanisms were characterized.

5.2.1. Wear Behavior

Wear can be a consequence of functional actions such as mastication or hygiene procedures as teeth brushing, considering particles from food intake or toothpaste that promote three-body abrasive wear of teeth or of restorative surfaces. Among the compounds often present in a tooth paste, there are abrasive particles, which warrant the removal of organic residues and biofilms. The most commonly used abrasive in tooth paste is the hydrated silica [11,169].

Representative wear marks obtained on VS from micro-abrasion tests in presence of distilled water containing or not abrasive particles are shown in Figure 5.11. The presence of abrasive particles promoted a substantial increase in the diameter of the wear mark after micro-abrasion tests, as seen in Figures 5.11A and C. This confirms the abrasive nature of hydrated silica particles as effective three-body agents [167].

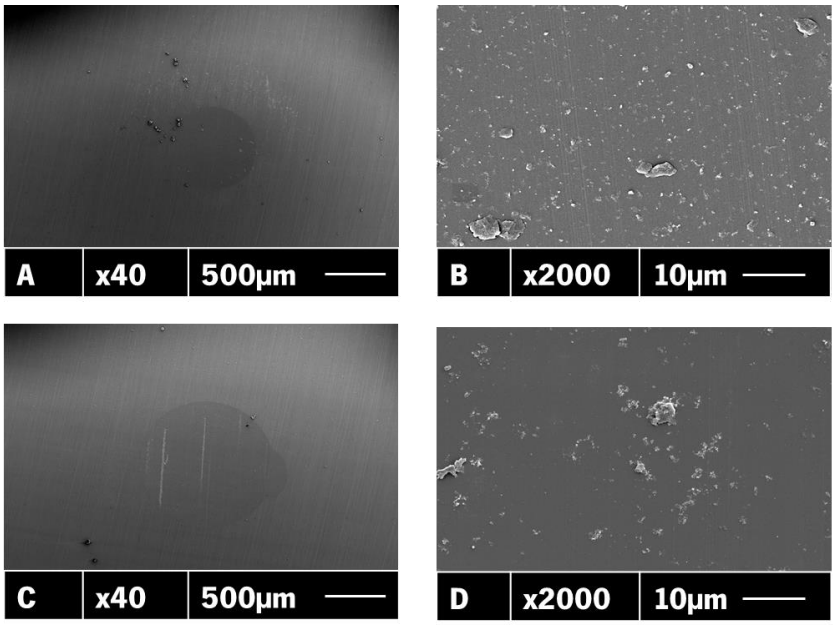

Figure 5.11: FEGSEM images of the VS worn surfaces after micro-abrasion tests under a load of 0.8 N (A and B) in presence of distilled water; and (C and D) in presence of slurry with 1/16 (%wt.) hydrated silica suspension.

The VS wear scar of the tests with hydrated silica, also presented wear outside the contact zone with the ball (Figure 5.11 (C)), which indicates that even without the effective applied load to the material surface, the abrasive particles of silica might also abrade the surface of the glass-ceramic.

In the wear mark, a smoother surface was noticed for VS samples in contact with abrasive slurries than that recorded for test surface in contact with distilled water free of abrasive particles. Thus, the abrasive silica particles not only increase the wear of VS samples, but also promote a polishing effect. However, a loosening of material is detrimental for the restorative structures considering occlusion and marginal fitting [130,170].

Representative wear marks obtained on VE samples after micro-abrasion tests in presence of distilled water containing or not abrasive particles are shown in Figure 5.12. After micro-abrasion tests, the diameter of the wear mark was larger on VE in contact with abrasive slurries (Fig. 5.12 C) than on one without abrasive (Fig. 5.12 A). VE surfaces were more susceptible to damage after micro-abrasion tests in distilled water containing or not abrasive when compared to VS samples [130,170].

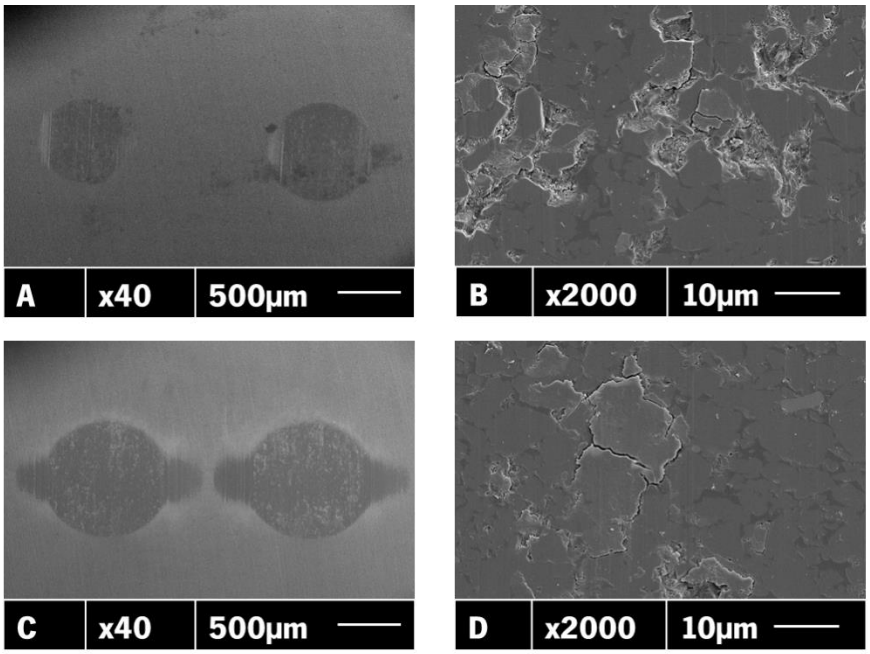

Figure 5.12: FEGSEM images of the VE worn surfaces after micro-abrasion tests under a load of 0.8 N, (A and B) in presence of distilled water; (C and D) in presence of slurry with 1/16 (%wt.) hydrated silica suspension.

The wear volume of VS and VE materials obtained from micro-abrasion tests are shown in Figure 5.13. VE revealed a statistically significant higher wear volume than that recorded for VS material, either on the situation with distilled water (C 0), or for the existence of particles of hydrated silica (C 1/16).

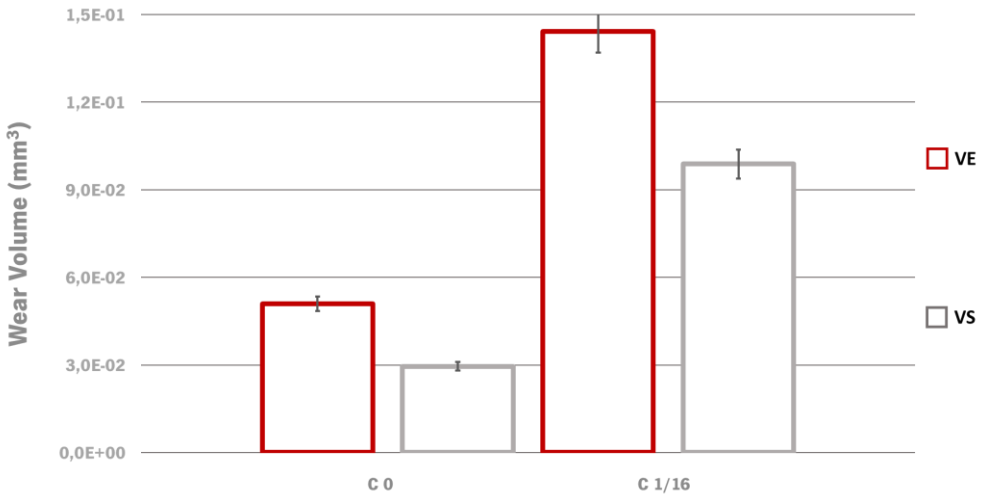

Figure 5.13: Volume loss of VS and VE in micro-abrasion tests with (C1/16) and without (C 0) abrasive particles (Fn=0,8 N).

These results, obtained from micro-abrasion tests, corroborate the results from the reciprocating sliding tests. VS and VE materials are of great interest, once they provide mechanical and optical properties closer to those of the human tooth. On the other hand, they have not yet been physically characterized by wear tests mimicking different oral conditions as performed in the present study. The study of wear become a common practice in dentistry, mainly due to the wide range of dental restorative materials available. Thus, the understanding of the wear mechanisms of VS and VE materials is the key to evaluate the long-term performance of these restorative structures in the oral environment.

A previous study reported similar mean values of wear volume of VS and VE against human enamel. Those results do not corroborate with the results obtained in the present work since the VE material showed a lower wear resistance both on the sliding and micro-abrasion tests, when compared with the VS samples. However, in that previous study, each material was prepared accordingly to the manufacturer guidelines, giving a different treatment to each material [171].

Some issues can be expected such as: the wide variety of in vitro wear tests following different parameters and the resulting difficulty in comparing among materials. Another problem is referent to the surface finishing of the test samples for wear tests.

Bogna et al. [172], compared the mechanical and optical properties of lithium disilicate and polymer-infiltrated glass-ceramics. The lithium disilicate glass-ceramics showed higher mechanical strength and aesthetic outcomes (namely discoloration rate and translucency) when compared to the polymer infiltrated ceramic. Although the use of different materials and following a different experimental procedure, results obtained in previous studies corroborate with the results obtained in the present study.

Comparing the results obtained in both tribological tests, it can be considered that they are in line with what is expected. In fact, for both tribological tests, the material VS, a zirconia-reinforced lithium disilicate glass-ceramic, presented higher wear resistance than the material VE, a polymer infiltrated ceramic.

6. CONCLUSIONS

6.1 Conclusions

Within the limitations of the reciprocating sliding and micro-abrasion test model used in the present work to mimic the oral cavity conditions, the main outcome of this work can be drawn as follows:

- The polymer-infiltrated ceramic network revealed an extensive running-in phase and unstable friction behavior against an alumina ball in a artificial saliva solution, with a higher dynamic friction coefficient, comparing with the same properties obtained for the zirconium lithium silicate glass-ceramic. The specific wear rate estimated for the polymer-infiltrated glass ceramic was almost two times higher than that recorded for the zirconium lithium silicate glass-ceramic after reciprocating wear sliding tests.
- During reciprocating sliding tests, abrasion with formation of tribo-layers was identified as the wear mechanisms for both test materials. Also, tribo-layers were thicker for the polymer-infiltrated ceramic than on the zirconium lithium silicate glass ceramic.

Regarding the abrasive wear tests made to evaluate the susceptibility to surface degradation involving contact in presence of abrasive slurry. The main outcomes of this part of the work can be drawn as follows:

- The wear volume with and without abrasive particles was statistically significantly higher for the polymer infiltrated glass ceramic than the volume lost by zirconia reinforced glass-ceramic.
- The presence of abrasive particles in suspension, causes polishing by a fine scale abrasion mechanism, in both materials.

Considering reciprocating wear sliding and micro-abrasion test results, the zirconium lithium silicate glass-ceramic showed a higher wear resistance than the polymer-infiltrated ceramic. In addition, zirconia reinforced glass-ceramic presented the lower friction coefficient values against alumina, thus putting in evidence the potential of application of this reinforced glass-ceramic in dental restorations.

6.2 Future Perspectives

Further studies should be performed on both zirconium lithium silicate and polymer infiltrated ceramic regarding the following issues:

- Concerning the variation in factors related to the oral conditions, there is room for future studies involving variation in loading, pH, temperature and abrasive particles.
- Since the tribological behavior of the materials are closely related to the surface finishing, it can be relevant to evaluate the influence of finishing procedures on the performance of different dental restorative materials;
- The tribological behavior of both materials should be evaluated by reciprocating sliding tests against natural human enamel and other ceramic materials (e.g. zirconia, ZLS or porcelain), to mimic other conditions as found *in vivo;*

REFERENCES

[1] Y.-S. Jung, J.-W. Lee, Y.-J. Choi, J.-S. Ahn, S.-W. Shin, J.-B. Huh, A study in the in vitro wear of the natural tooth structure by opposing ziconia or dental porcelain, J. Adv. Prosthodont. 2 (2010) 111–115.

[2] R.W. Phillips, Mechanical Properties of Dental Materials, Phillip's Sci. Dent. Mater. (2011) 1–11. http://www.webdental.com/profiles/blogs/mechanical-poperties-of (accessed October 12, 2016).

[3] M.K. Al-Omiri, M.G. Sghaireen, B.K. Alzarea, E. Lynch, Quantification of incisal tooth wear in upper anterior teeth: Conventional vs new method using toolmakers microscope and a three-dimensional measuring technique, J. Dent. 41 (2013) 1214–1221.

[4] Z.R. Zhou, J. Zheng, Tribology of dental materials: a review, J. Phys. D. Appl. Phys. 41 (2008) 113001.

[5] P. Lambrechts, K. Goovaerts, D. Bharadwaj, J. De Munck, L. Bergmans, M. Peumans, B. Van Meerbeek, Degradation of tooth structure and restorative materials : A review, Wear. 261 (2006) 980–986.

[6] K.J. Anusavice, C. Shen, H.R. Rawls, Phillips' Science of Dental Materials, 2013.

[7] W.S. Oh, R. DeLong, K.J. Anusavice, Factors affecting enamel and ceramic wear: A literature review, J. Prosthet. Dent. 87 (2002) 451–459. doi:10.1067/mpr.2002.123851.

[8] S.D. Heintze, How to qualify and validate wear simulation devices and methods, Dent. Mater. 22 (2006) 712–734.

[9] C. de Villiers, T. Scriba, The History of Dentistry, Namibia Dent. Assoc. (2016). http://www.namibiadent.com/the-history-of-dentistry.html (accessed November 24, 2016).

[10] B.D. Ratner, A.S. Hoffman, F.J. Schoen, J.E. Lemons, Biomaterials Science, 1996.

[11] Z. Zhou, Z. Jin, Biotribology: recent progresses and future perspectives, Elsevier, Biosurface and Biotribology. 1 (2015) 3–24.

[12] ISO, ISO/ TC 106: Wear; Terms, Systematic Analysis of Wear Processes, Classification of Wear Phenomena, (2011).

[13] I. Denry, J.R. Kelly, Emerging Ceramic-based Materials for Dentistry, J. Dent. Res. 93 (2014) 1235–42.

[14] R.N. Raghavan, Ceramics in Dentistry, in: Sinter. Ceram. - New Emerg. Tech., 2012: pp. 203–224.

[15] S. Santander, F. Monteiro, Ceramics for dental restorations - An Introduction, 2010.

[16] A. Shenoy, N. Shenoy, Dental ceramics: An update, J. Conserv. Dent. 13 (2010) 195–203.

[17] I.L. Denry, Recent advances in ceramics for dentistry, Crit Rev Oral Biol Med. 7 (2016) 134–143.

[18] R. AS, Jones DW, Indentation fracture toughness and dynamic elastic moduli for commercial feldspathic dental porcelain materials, Dent. Mater. 20 (2004) 198–206.

[19] J.R. Lovadino, R. Sano, S. Terada, R.C. Pascotto, Advances in dental veneers : materials , applications , and techniques, Clin. Cosmet. Investig. Dent. 4 (2012) 9–16.

[20] L.H. Mair, T.A. Stolarski, R.W. Vowles, C.H. Lloyd, Wear: Mechanisms, manifestations and measurement. Report of a workshop, J Dent Res. 24 (1996) 141–148.

[21] V.P. Thompson, Performance of Dental Ceramics : Challenges for Improvements, J Dent Res. 90 (2011) 937–952. doi:10.1177/0022034510391795.

[22] P. Lambrechts, E. Debels, K. Van Landuyt, M. Peumans, B. Van Meerbeek, How to simulate wear ? Overview of existing methods, Dent. Mater. 22 (2006) 693–701.

[23] M. Nelson Stanley, Wheeler's Dental Anatomy, Phisiology and Occlusion, Saunders Elsevier, Missouri:, 2010.

[24] J. Regan, C. Vanputte, A. Russo, Seeley's Essentials of Anatomy & Physiology, 2016.

[25] Dental quadrants, Wikimedia Commons. (n.d.). https://commons.wikimedia.org/wiki/File:Dental_quadrants.png.

[26] Structure and organization of human dentition, (n.d.). http://www.helsinki.fi/science/dentgen/h_eng.gif.

[27] L. Junqueira, J. Carneiro, Histologia Básica., Editora Guanabara Koogan, Rio de Janeiro, 2008.

[28] A. Nanci, Histologia Oral: desenvolvimento, estrutura e função, Elsevier, 2008.

[29] D. Ramirez, Endodoncia, Clin. Dent. Dr. Fuentes. (n.d.). https://s3.amazonaws.com/classmint.img/23e5e0d0-771c-40fe-a6ef-9ace8df4640e.jpeg.

[30] J. Hunter, F.C. Webb, R.T. Hulme, The Human Teeth, 192nd ed., London, 1863.

[31] A.G. Fincham, The Structural Biology of the Developing Dental Enamel Matrix, J. Struct. Biol. (1999) 270–299.

[32] M. Hoffman, The Teeth (Human Anatomy), Pict. Teeth. (2017) 5–10. http://www.webmd.com/oral-health/picture-of-the-teeth#1 (accessed May 17, 2017).

[33] A.B. Michel Goldberg, Dentin: Structure, Composition and Mineralization: The role of dentin ECM in dentin formation and mineralization, Front Biosci. (2012) 711–735.

[34] K.J. Anusavice, W.A. Brantley, Physical properties of dental materials, in: K.J. Anusavice (Ed.), Phillip's Sci. Dent. Mater., Saunders, St. louis, 2003: pp. 42–71.

[35] H.H. Xu, D.T. Smith, S. Jahanmir, E. Romberg, J.R. Kelly, V.P. Thompson, E.D. Rekow, Indentation damage and mechanical properties of human enamel and dentin., J Dent Res. 77 (1998).

[36] V. Imbeni, J.J. Kruzic, G.W. Marshall, S.J. Marshall, R.O. Ritchie, The dentin–enamel junction and the fracture of human teeth, Nat. Mater. 4 (2005) 229–232.

[37] S.J. Marshall, M. Balooch, S. Habelitz, G. Balooch, R. Gallagher, G.W. Marshall, The dentin – enamel junction — a natural, multilevel interface, J. Eur. Ceram. Soc. 23 (2003) 2897–2904.

[38] V. IMBENI, J.J. KRUZIC, G.W. MARSHALL, S.J. MARSHALL, R.O. RITCHIE, The dentin–enamel junction and the fracture of human teeth, Nat. Mater. 4 (2005) 94720.

[39] P. Zaslansky, A.A. Friesem, S. Weiner, Structure and mechanical properties of the soft zone separating bulk dentin and enamel in crowns of human teeth : Insight into tooth function, J. Struct. Biol. 153 (2006) 188–199.

[40] W. Hylander, W.L. Hylander, Temporomandibular Joint, in: Funct. Anat. Biomech. Masticatory Appar., 2014: pp. 2–34.

[41] V.D. Stejskal, A. Danersund, A. Lindvall, R. Hudecek, V. Nordman, Y. A., W. Mayer, W. Bieger, U. Lindh, Metal-specific lymphocytes: biomarkers of sensitivity in man, Neuro Endocrinol Lett. 20 (1999) 289–298.

[42] J.D. Bumgardner, L.C. Lucas, Cellular Response to Metallic Ions Released from Nickel-Chromium Dental Alloys, J. Dent. Res. 74 (1995) 1521–1527.

[43] S. Santander, F. Monteiro, Ceramics for Dental Restorations – an Introduction, Medellin. 77 (2010) 26–36.

[44] M. A.Rosenblum, A. Schulman, A Review of All-Ceramic Restorations, J. Am. Dent. Assoc. 128 (1997) 297–307.

[45] L. Duzdar, M. Oksuz, I. Tanboga, Evaluation of the Bond Strength of Resin Cements Used to Lute Ceramics on Laser-Etched Dentin, Photomed. Laser Surg. 32 (2014) 413–421.

[46] P. Magne, U. Belser, Restaurações adesivas de porcelana na dentição anterior: uma abordagem biomimética, Quintessence Int. (Berl). (2003).

[47] P.V. Soares, P. Henrique, R. Spini, D.D.S. Valessa, F. Carvalho, P. Gomes, S. Ramon, C. De Queiroz, G. Andrea, B. Tolentino, D.D.S.A. Coelho, Aesthetic rehabilitation with laminated ceramic veneers reinforced by lithium disilicate, Quintessence Int. (Berl). 45 (2014) 129–133.

[48] J.R. Kelly, P. Benetti, Ceramic materials in dentistry : historical evolution and current practice, Aust. Dent. J. 56 (2011) 84–96.

[49] D.W. Jones, Development of dental ceramics. An historical perspective, Dent Clin North Am. 29 (1985) 62144.

[50] L.H.A. Raposo, L.R. Davi, P.C.S. Júnior, F.D. das Neves, P.V. Soares, V.R.N. Simamoto, A.C. Machado, A.G. Pereira, P.S. Borella, Restaurações Totalmente Cerâmicas : Características, Aplicações clínicas e longevidade, in: Pro-Odonto Prótese E Dentística, 2012: pp. 9–74.

[51] E.A. Gomes, E.P. Rocha, P.H. Santos, Cerâmicas odontológicas : o estado atual (Ceramic in dentistry : current situation), Cerâmica. 54 (2008) 319–325.

[52] H. Conrad, W. Seong, I. Pesun, Current ceramic materials and systems with clinical recommendations : a systematic review ., J Prosthet Dent. 98 (2017) 1–2.

[53] C. RJ, J. Simonsen, Effect of coupling agents on bond strenght of etched porcelain, J Dent Res. 63 (1984) 179.

[54] P.J. Babu, R.K. Alla, V.R. Alluri, S.R. Datla, Dental Ceramics: Part I – An Overview of Composition , Structure and Properties, Am. J. Mater. Eng. Technol. 3 (2015) 13–18.

[55] J.W. McLean, T.H. Hughes, The reinforcement of dental porcelain with ceramic oxides, Br Dent J. 119 (2017) 251–267.

[56] I. Denry, J.A. Holloway, Ceramics for Dental Applications: A Review, Materials (Basel). 3 (2010) 351–368. doi:10.3390/ma3010351.

[57] F. Dental, ENDODONTICS CAD CAM, CAD CAM RESTORATIONS. (2016) 1. http://www.fmsdental.com/endodontics-cad-cam/.

[58] C. EN, Restaurações Estéticas: Compósitos, Cerâmicas e Implantes Artes Médicas, São Paulo, 2005.

[59] R. Giordano, E.A. McLaren, Ceramics overview: classification by microstructure and processing methods, Compend Contin Educ Dent. 31 (2010) 682–684.

[60] A. Della Bona, J.R. Kelly, The clinical success of all-ceramic restorations, J Am Dent Assoc. 138 (2008) 8S–13S.

[61] L. D., W. T., An up to 16-year prospective study of 304 porcelain veneers, Int J Prosthodont. 20 (2007) 389–396.

[62] R. Wai, K. Li, M. Uk, M. Ed, T.W. Chow, F. Fadm, J.P. Matinlinna, C.A.D. Cam, ScienceDirect Ceramic dental biomaterials and CAD / CAM technology : State of the art, J. Prosthodont. Res. 58 (2014) 208–216.

[63] S. F., H. J., Which all-ceramic system is optimal for anterior for anterior aesthetics?, J Am Dent Assoc. 139 (2008) 19S–24S.

[64] P. Guess, S. Schultheis, E. Bonfante, P. Coelho, All-ceramic systems: laboratory and clinical performance, Dent Clin North Am. 55 (2011) 333–352.

[65] Z.H.R.G.& Co.KG, Vita suprinity ® The Concept, (2015) 2–20.

[66] M. Fradeani, M. D'Amelio, M. Redemagni, M. Corrado, Five-year follow-up with Procera all-ceramic crowns, Quintessence Int. (Berl). 36 (2005) 105–113.

[67] F. M, R. M, An 11-year clinical evaluation of leucite-reinforced glass-ceramic crowns: a retrospective study, Quintessence Int. (Berl). 33 (2002) 503–510.

[68] U. Pallesen, J.W. van Dijken, An 8-year evaluation of sintered ceramic and glass ceramic inlays processed by the Cerec CAD/CAM system, Eur J Oral Sci. 108 (2000) 239–246.

[69] G. Sjogren, R. Lantto, A. Granberg, B.O. Sundstrom, A. Tillberg, Clinical examination of leucite-reinforced glass-ceramic crowns (Empress) in general practice: a retrospective study, Int J Prosthodont. 12 (1999) 122–128.

[70] P.V. von Steyern, O. Jonsson, K. Nilner, Five-year evaluation of posterior all-ceramic three-unit (In-Ceram) FPDs, Int J Prosthodont. 14 (2001) 379–384.

[71] S. Wolfart, F. Bohlsen, S.M. Wegner, M. Kern, Preliminary prospective evaluation of all-ceramic crown-retained and inlay-retained fixed partial dentures, Int J Prosthodont. 18 (2005) 497–505.

[72] A. Bindl, W.H. Mörmann, An up to 5-year clinical evaluation of posterior in-ceram CAD/CAM core crowns, Int J Prosthodont. 15 (2002) 451–456.

[73] Probster L, Four year clinical study of glass-infiltrated, sintered alumina crowns, J Oral Rehabil. 23 (1996) 147–151.

[74] L. He, M. Swain, C.A.D. Cam, A novel polymer infiltrated ceramic dental material, Dent. Mater. 27 (2011) 527–534.

[75] C. Dirxen, U. Blunck, S. Preissner, Clinical Performance of a New Biomimetic Double Network Material, Open Dent. J. 7 (2013) 118–122.

[76] M.G. Wiesli, M. Özcan, High-Performance Polymers and Their Potential Application as Medical and Oral Implant Materials: A Review, (2015) 1–24.

[77] J.F. Guth, E.S.J.S. Almeida, M. Ramberger, F. Beuer, D. Edelhoff, Treatment concept with CAD/CAM-fabricated high-density polymer temporary restorations, J Esthet Restor Dent. 24 (2012) 310–318.

[78] A. V, C. M., Clinical study of direct composite fullcoverage crowns: long-term results, Oper Dent. 37 (2012) 432–441.

[79] S. Preissner, E. Kostka, U. Blunck, A noninvasive treatment of amelogenesis imperfecta., Quintessence Int. (Berl). 44 (2013) 303–305.

[80] S. S.Mantri, A.S. Bhasin, CAD/CAM in dental restorations: an overview, J. Ann. Essences Dent. 2 (2010) 123–128.

[81] J.G. Wittneben, R.F. Wright, H.P. Weber, G.O. Gallucci, A systematic review of the clinical performance of CAD/CAM single-tooth restorations, Int J Prosthodont. 22 (2009) 446–471.

[82] W.H. Mörmann, M. Brandestini, Cerec-System: computerized inlays, onlays and shell veneers, Zahnarztl Mitt. 77 (1987) 2400–2405.

[83] G. Davidowitz, P.G. Kotick, The use of CAD/CAM in Dentistry, Dent Clin North Am. 55 (2011) 559–570.

[84] P.-R. Liu, A Panorama of Dental CAD/CAM Restorative Systems, J. Compend. 26 (2005) 507–512.

[85] N. Shrivastava, CAD/CAM and CAD/CIM in restorative dentistry, Conserv. Dent. Endod. (2015) 85. https://pt.slideshare.net/drnids_modern/cad-cam-and-cadcim-in-restorative-dentistry (accessed October 15, 2017).

[86] D.G. Grossman, Machinable glass-ceramic based on tetrasilicic mica, J. Am. Ceram. Soc. 55 (1972) 446–449.

[87] F. Duret, J.L. Blouin, B. Duret, CAD-CAM in dentistry, J. Am. Dent. Assoc. 117 (1988) 715–720.

[88] J. Tinschert, G. Natt, S. Hassenpflug, Status of current CAD/CAM technology in dental medicine, Int. J. Comput. Dent. 7 (2004) 25–45.

[89] B. Rosca, S. Ramalho, J.C. Sampaio-fernandes, Reparability of two different CAD / CAM polymer materials using a light-cured composite and universal adhesives, Soc. Port. Estomatol. E Med. Dentária. 7 (2016) 189–196.

[90] Zahnfabrik H. Rauter GmbH & Co.KG, Vita Enamic - Technical and scientific documentation, 2013.

[91] A. Della, P.H. Corazza, Y. Zhang, Characterization of a polymer-infiltrated ceramic-network material, Dent. Mater. 30 (2014) 564–569.

[92] A. Shenoy, N. Shenoy, Dental Ceramics: an update, J. Conserv. Dent. 13 (2010) 195–203.

[93] F. Beuer, J. Schweiger, D. Edelhoff, Digital dentistry : an overview of recent developments for CAD / CAM generated restorations, (n.d.) 505–511.

[94] B. Bhushan, Principles and Applications of Tribology, 2013.

[95] B. Bhushan, Modern tribology handbook, 2001.

[96] S.J. Shaffer, Tribology 101 – Introduction to the Basics of Tribology, (2013) 67.

[97] B. Bhushan, Introduction to Tribology, John Wiley & Sons, 2002. https://books.google.pt/books?id=U9er18cvVeEC&dq=tribology++historic+contextualization&hl=pt-PT&source=gbs_navlinks_s.

[98] M.H. Müser, Lectures and notes of physics, (2002) 289–317.

[99] K.-H. Zum Gahr, Microstructure and Wear of Materials, Elsevier Science Publishers B.V., New York, 1987.

[100] H.P. Jost, Lubrication (tribology) education and research, 1966.

[101] M.B. Petersen, W.O. Winer, Wear Control Handbook, New York, 1980.

[102] A. Martini, Introduction to Tribology, Soc. Tribol. Lubr. Eng. (2017). http://www.stle.org/files/What_is_tribology/Tribology.aspx.

[103] Mati paasuke, Biomechanics of the knee joint Table of contents, Biomech. Present. (2011) 244.

[104] H. Kahn, Preface to the viewpoint set: Materils issues in MEMS, Scr. Mater. 59 (2008) 909–911.

[105] M. Urbakh, J.K.D.G.J. Israelachvilli, The nonlinear nature of friction, Nature. 430 (2004) 525–528.

[106] DIN, DIN 50320: Wear; Terms, Systematic Analysis of Wear Processes, Classification of Wear Phenomena, (1979).

[107] H. Czichos, Introduction to friction and wear, in: F. K. (Ed.), Frict. Wear Polym. Compos., Elsevier, Amsterdam, 1986: pp. 1–22.

[108] G. Stachowiak, A.W. Batchelor, Engineering Tribology, Butterworth-Heinemann, 2013.

[109] T. Mang, K. Bobzin, T. Bartels, Industrial Tribology: Tribosystems, Friction, Wear and Surface Engineering, Lubrication, John Wiley & Sons, 2011.

[110] I.M. Hutchings, Tribology - Friction and wear of engineelring materials, Edward Arnold Press, London, 1992.

[111] S. Wen, P. Huang, Principles of Tribology, John Wiley & Sons, 2012.

[112] A.S. Miranda, Noções básicas de Tribologia, Guimarães, n.d.

[113] K. Holmberg, A. Matthews, Coatings Tribology: Properties, Mechanisms, Techniques and Applications in Surface Engineering, Elsevier, 2009.

[114] B.T.W.G. Miranda-júnior, R.P.J.T.M. Oda, Surface Roughness in Ceramics with Different Finishing Techniques Using Atomic Force Microscope and Profilometer, Oper. Dent. 31 (2006) 442–449.

[115] Z.R. Zhou, Z.M. Jin, Biotribology: recent progresses and future perspectives, Biosurface and Biotribology. 1 (2015) 3–24.

[116] J. Zheng, Z. Zhou, Friction and wear behavior of human teeth under various wear conditions, Tribiology Int. 40 (2007) 278–284.

[117] Dentodontics, Tooth Wear. (2015) 1. https://dentodontics.com/2015/12/21/tooth-wear/ (accessed November 17, 2017).

[118] S.M. Hooper, R.G. Newcombe, R. Faller, S. Eversole, M. Addy, N.X. West, The protective effects of toothpaste against erosion by orange juice : Studies in situ and in vitro, J. Dent. 35 (2007) 476–481.

[119] B.T. Amaechi, S.M. Higham, Dental erosion: possible approaches to prevention and control, J Dent Res. 33 (2005) 243–252.

[120] R. Lewis, R.S. Dwyer-Joyce, Wear of human teeth: A tribological perspectiv, J. Eng. Tribol. 219 (2005) 1–18.

[121] E.D. C.C., Human tooth wear in the past and the present: Tribological mechanisms, scoring systems, dental and skeletal compensations., Arch. Oral Biol. (2012) 214–229.

[122] S. Hooper, W. Nx, P. Mj, A. Joiner, N. Rg, A.M. Investigation, Investigation of erosion and abrasion on enamel and dentine : a model in situ using toothpastes of different abrasivity,

J. Clin. Periondontology. 30 (2003) 802–808.

[123] M. Addy, M.L. Hunter, Can tooth brushing damage your health ? Effects on oral and dental tissues, Int. Dent. J. 53 (2003) 177–186.

[124] C. Ganss, M. Hardt, D. Blazek, J. Klimek, S.N. Effects, C. Ganss, M. Hardt, D. Blazek, J. Klimek, N. Schlueter, Effects of toothbrushing force on the mineral content and demineralized organic matrix of eroded dentine, Eur. J. Oral Sci. (2009) 255–260.

[125] V. Çanakçi, A. Tezel, Clinical Evaluation of an Paste Containing Stannous Hypersensitivity Following Toothbrush with Fluoride in Treatment of Dentine Periodontal Surgery a Tooth Recep ORBAK , Varol CANAKCI and Adnan TEZEL Department of Periodontology , Faculty of Dentistry , T, Dent. Mater. J. 20 (2001) 164–171.

[126] S. Kumar, J. Panwar, J. Sharma, B. Goutham, P. Duraiswamy, S. Kulkarni, Tooth cleaning frequency in relation to socio-demographic variables and personal hygiene measures among school children of Udaipur district , India, Int. J. Dent. Hyg. 9 (2011) 3–8.

[127] R.. Boyd, L. McLey, R. Zahradnik, Clinical and Laboratory Evaluation of Powered Electric Toothbrushes : In Vivo Determination of Average Force for Use of Manual and Powered Toothbrushes, J. Clin. Dent. 8 (1997) 2017.

[128] F.G. Burgett, M.M. Ash, Comparative Study of the Pressure of Brushing with Three Types of Toothbrushes, J. Periodontol. 45 (1974) 410–413.

[129] C. Ganss, N. Schlueter, S. Preiss, J. Klimek, Tooth brushing habits in uninstructed adults — frequency , technique , duration and force, Clin Oral Invest. 13 (2009) 203–208.

[130] A. Wiegand, J. Patrik, M. Burkhard, F. Eggmann, T. Attin, Brushing force of manual and sonic toothbrushes affects dental hard tissue abrasion, Clin Oral Invest. 17 (2013) 815–822.

[131] L. WebMD, WebMD, Too Much Press. or Time Brushing Your Teeth Can Hurt. (2017) 1–6. https://www.webmd.com/oral-health/news/20030620/go-easy-toothbrush (accessed May 16, 2017).

[132] P. Heasman, BBC News, Brushing Too Hard â€™ Damages Teeth ’. (2017) 1–2. http://news.bbc.co.uk/2/hi/health/2999806.stm (accessed May 16, 2017).

[133] J. Zheng, Z.R. Zhou, Effect of age on the friction and wear behaviors of human teeth, Tribiology Int. 39 (2006) 266–273.

[134] R. Lewis, R. Dwyer-Joyce, Wear of human teeth: a tribological perspective., Part J J. Eng. Tribol. 219 (2005) 1–18.

[135] A. Lussi, T. Jaeggi, Erosion - diagnosis and risk factors, Clin. Oral Investig. 12 (2008) 5–13.

[136] J.C.M. Souza, M. Henriques, W. Teughels, P. Ponthiaux, J.-P. Celis, L.A. Rocha, Wear and Corrosion Interactions on Titanium in Oral Environment: Literature Review, . Bio- Tribo-Corrosion. 1 (2015) 13.

[137] T. Imfeld, Dental erosion. Definition, classification and links, Eur. J. Oral Sci. 104 (1996) 151–155.

[138] L.H. Mair, R.W. Vowles, C.H. Lloyd, Wear : mechanisms , manifestations and measurement . Report of a workshop, 24 (1996) 141–148.

[139] J. Zheng, Nanomechanical properties and microtribological behaviours of human tooth enamel, Part J J. Eng. Tribol. 224 (2010) 577–587.

[140] H.Y. Yu, Z.B. Cai, P.D. Ren, M.H. Zhu, Z.R. Zhou, Friction and wear behavior of dental feldspathic porcelain, Wear. 261 (2006) 611–613.

[141] J.A. Arsecularatne, M. Hoffman, Ceramic-like wear behaviour of human dental enamel, J. Mech. Behav. Biomed. Mater. 8 (2012) 47–57.

[142] Z.H.R.G.& Co.KG, Vita Suprinity ® Technical and scientific documentation, 2001. http://vitanorthamerica.com//wp-content/uploads/2013/10/VITA_2001E_SUPRINITY_PS_EN_V01_.pdf.

[143] ISO, ISO 6872: Dentistry - Ceramic Materials, (2015) 28.

[144] O. Rubem, K. Montedo, F.J. Floriano, J.D.O. Filho, A.M. Bernardin, Sintering Behavior of LZSA Glass-Ceramics, Mater. Res. 12 (2009) 197–200.

[145] S.E. Elsaka, A.M. Elnaghy, Mechanical properties of zirconia reinforced lithium silicate glass-ceramic, Dent. Mater. 2 (2015) 908–914.

[146] ISO, ISO 10477: Dentistry - Polymer-based crown and bridge materials, (2004) 21.

[147] B.G.N. Smith, J.K. Knight, An index for measuring tooth wear, Br Dent J. 156 (1984) 435–438.

[148] C.M. Souza, P. Ponthiaux, M. Henriques, R. Oliveira, W. Teughels, J.-P. Celis, L. Rocha, Corrosion behaviour of titanium in the presence of Streptococcus mutans, J. Dent. 41 (2013) 528–534.

[149] Y. Imai, S. Suzuki, S. Fukushima, Enamel wear of modified porcelains, Am J Dent. 13 (2000) 315–323.

[150] A.C. Faria, A.A. Oliveria, E.A. Gomes, R.C. Rodriges, R.F. Ribeiro, Wear resistance of pressable low fusing ceramic opposed by dental alloys, J Mech. Behav. Biom. Mater. 32 (2014) 40–51.

[151] A.C.F. Bentes, Desgaste de Materiais Dentários de Restauro Direto, Universidade do Minho, 2014.

[152] M.Â.G. Sampaio, J.M.R. Gomes, J.C.M. de Souza, Wear of PEEK / Ti6Al4V systems under micro-abrasion and linear sliding conditions, University of Minho, 2015.

[153] Z. Doni, A.C. Alves, F. Toptan, J.R. Gomes, A. Ramalho, M. Buciumeanu, L. Palaghian, F.S. Silva, Dry sliding and tribocorrosion behaviour of hot pressed CoCrMo biomedical alloy as compared with the cast CoCrMo and Ti6Al4V alloys., Mater. Des. 52 (2013) 47–57.

[154] J.A. Arsecularatne, J.P. Dingeldein, M. Hoffman, An in vitro study of the wear mechanism of a leucite glass dental ceramic, Biosurface and Biotribology. 1 (2015) 50–61.

[155] M.J. Neale, The Tribology Handook, 2nd ed., 2001.

[156] J.A. Arsecularatne, N.R. Chung, M. Hoffman, An in vitro study of the wear behaviour of dental composites, Biosurface and Biotribology. 2 (2016) 102–113.

[157] W.H. Douglas, R.L. Sakaguchi, R. Delong, Frictional effects between natural teeth in an artificial mouth, Dent. Mater. 1 (1985) 115–119. http://www.demajournal.com/article/S0109-5641(85)80040-3/abstract 1/2.

[158] Z. Xu, P. Yu, D.D. Arola, J. Min, S. Gao, A comparative study on the wear behavior of a polymer infiltrated ceramic network (PICN) material and tooth enamel, Dent. Mater. 3 (2017) 1351–1361.

[159] P.V. Antunes, A. Ramalho, Study of abrasive resistance of composites for dental restoration by ball-cratering, Wear. 255 (2003) 990–998.

[160] I.M. Hutchings, Tribology: Friction and Wear of Engineering Materials, Butterworth-Heinemann, 1992.

[161] H.P. Jost, Tribology: How a word was coined 40 years ago., Tribol. Lubr. Technol. (2006) 24–29.

[162] W.H. Mörmann, B. Stawarczyk, A. Ender, B. Sener, T. Attin, A. Mehl, Wear characteristics of current aesthetic dental restorative CAD / CAM materials : Two-body wear , gloss retention , roughness and Martens hardness, J. Mech. Behav. Biomed. Mater. 20 (2013) 113–125.

[163] E. Elhomiamy, Y. Aboushady, B. El Malakh, Wear behaviour and surface roughness of Polymer infiltrated ceramic material Compared to pressable glass ceramic, Dent. News (Lond). (2017) 1–12. http://www.dentalnews.com/2017/02/08/wear-behaviour-surface-roughness-polymer-infiltrated-ceramic-material-compared-pressable-glass-ceramic (accessed November 12, 2017).

[164] B. Stawarczyk, A. Liebermann, M. Eichberger, J.F. Guth, Evaluation of mechanical and optical behavior of current aesthetic dental restorative cad/cam composites, J Mech Behav Biomed Mater. 55 (2015) 1–11.

[165] C.L. Nathaniel, B. Ritika, O.B. John, Wear , strength , modulus and hardness of CAD / CAM restorative materials, Dent. Mater. 32 (2016) e275–e283.

[166] H. El Zhawi, M.R. Kaizer, A. Chughta, R.R. Moraes., Y. Zhang, Polymer Infiltrated Ceramic Network Structures for Resistance to Fatigue Fracture and Wear, Dent Mater. 32 (2017) 1352–1361.

[167] M.V. Swain, A. Coldea, A. Bilkhair, P.C. Guess, Interpenetrating network ceramic-resin composite dental restorative materials, Dent Mater. 32 (2015) 34–42.

[168] T. Miyazaki, Y. Hotta, J. Kunii, S. Kuriyama, Y. Tamaki, A review of dental CAD / CAM : current status and future perspectives from 20 years of experience, 28 (2009) 44–56.

[169] R. Davies, C. Scully, A. Preston, Dentifrices - an update, Med. Oral Patol. Oral Y Cir. Bucal. 15 (2010) e976–e982.

[170] E.B. Bhushan, J.A. Harrison, S.J. Stuart, Atomic-Scale Simulation of Tribological and Related Phenomena, in: Handb. Micro/Nanotribology, 1999: pp. 1–71.

[171] E.A. Naumova, S. Schneider, W.H. Arnold, A. Piwowarczyk, Wear Behavior of Ceramic CAD/CAM Crowns and Natural Antagonists, Materials (Basel). 10 (2017) 1–13.

[172] B. Stawarczyk, A. Liebermann, M. Eichberger, J. Gu, C.A.D. Cam, Evaluation of mechanical and optical behavior of current aesthetic dental restorative CAD / CAM composites, J. Mech. Behav. Biomed. Mater. 55 (2016) 1–11.